

Chapter 4

Bio-Microfluidics: Overview

Coupling Biology and Fluid Physics at the Scale of Microconfinement

Tamal Das and Suman Chakraborty

Abstract With a view to establish unique interfacial synergistic interactions between two seemingly distant fields of microfluidics and biology, Bio-microfluidics has become a progressive arena of research in recent times. Bio-microfluidic tools in the format of lab-on-a-chip devices have been extensively utilized to uncouth hitherto un-illuminated regions of cellular-molecular biology, biotechnology and biomedical engineering. This chapter elaborately delineates the linking between the fundamental microscale physics and biologically relevant physico-chemical events and how, in practice, these relations are exploited in microfluidic devices. Finally, potential directions of future biomicrofluidic research are also discussed.

Keywords Lab-on-a-chip · Micro Total Analysis System · Micro-fabrication · Microchannel · Combinatorial Chemistry · Micromixing · Microarray · Cellomics · Genomics · Proteomics · Diffusion · Dispersion · Drug Delivery · Microneedle · Polymerase Chain Reaction · Field-Flow Fractionation · Reaction Kinetics · Enzyme Assay · Electroosmosis · Electro-wetting · Dielectrophoresis · Electrophoresis · Ferrofluid · Fluorescence · Microscopy · Confocal Microscopy · Optofluidics · Flow Visualization · Biosenor · Structural Biology · Capillary · Electrophoresis

4.1 Introduction

Microfluidics deals with the transport of minute volumes of fluid (typically, sub-nanoliter) through channels having at least one of three dimensions of the order of micrometer [1]. Though, initially microfluidics stemmed out of two distant fields, namely, analytical chemistry [2] and microfabrication [3], soon potentials of the subject were to be unleashed in the field of biology [4]. During the past few years, its

S. Chakraborty (✉)
Department of Mechanical Engineering, Indian Institute of Technology, Kharagpur,
Kharagpur-721302, India
e-mail: suman@mech.iitkgp.ernet.in

scope has stretched beyond exploring exotic transport phenomena and low Reynolds number fluid physics into the domains of biochemical analysis [5, 6]. The urgency of invoking microfluidic devices in solving relevant chemical and biochemical problems has been obviated because of two major beneficiaries that they have in promise. First, within microfluidic confinements, the assay volume requirement of liquid analytes has been discovered to be unprecedentedly low. Second, due to its intrinsic augmented surface area to volume ratio over reduced length scales, microfluidic devices can offer enhanced throughput, reduced reaction time and higher sensitivity [7, 8]. Subsequently, adopting microfluidics in biology has revolutionized the paradigms of molecular biology, biochemistry and bioengineering in such a unanimous extent that relevant fundamental science and applications are classified by the researchers under the tenet of a separate subject hailed Biomicrofluidics [4]. The initial flourish of Biomicrofluidics has been facilitated by the expanding the necessity of achieving faster and high throughput Genomics during the past decades [9]. However, in post genomic era, Biomicrofluidics based applications seem to sprout everywhere in the vistas. Its spectrum encompassed vast bio-domains ranging from cell biology [10] to protein crystallization [11], from nucleic acid isolation [12–14] to lethal virus detection [15]. Now, the subject has become progressive enough to miniaturize bulk of the analytical experiments performed in laboratory scale within few square centimeter space of a monolithic platform and specific jargons such as Lab-on-a-Chip (LoC) and micro Total Analysis Systems (μ TAS) have become cliché in the scientific world [16–18]. Microfluidic systems have been demonstrated to possess potential in diverse spectra of biological applications, encompassing molecular separations, enzymatic assays [19], polymerase chain reactions [20], and immunohybridization reactions [21]. These are outstanding individual instances of down-scaled methods of laboratory techniques, but there also exist stand-alone functionalities, analogous to a single component integrated circuit. Given that the present day industrial approaches to address pertinent large-scale biological integration have emerged in the form of gigantic robotic based fluidic platforms which consume substantial space and expenses, Biomicrofluidics has a straightway objective of replacing them with powerful miniaturization [6]. This way, its projected functionalities are quite similar to the silicon based intergrated circuit that replaced spacious valve-devices during VLSI (Very Large Scale Integration) chip revolutions of computation industry.

The very purpose of microfluidics devices is to deal with samples often dissolved in an aqueous phase and then, manipulate the system through characteristic analytical procedures such as heating, mixing and separation. Subsequently, processed solutions may be transported to some form of a detector or sensor and the data is acquired. Microfluidic channel networks [22], generally and economically fabricated in a monolithic platform [23] made of a moldable silicon based polymer such as Polydimethylsiloxane (PDMS) or glass, include features such as separators, mixers, valves and injectors which are essentially microscale counterparts of existing macroscale analytical and bioreactor process components. However, in an inexpensive mode, microchannel networks may be fabricated in compact disc like platform and therein, fluid flows may be actuated by centrifugal and coriolis forces

[24, 25]. Once the device has been designed and manufactured, what becomes indispensable here is to achieve apposite micro-macro interfacial connections to user accessible macroscale input-output components. The microfluidic technology in-complemented with macroscale interface, permits the consistent maneuvering of small sample volume with ensured reproducibility and accuracy.

Two of the most early Biomicrofluidics appliances were microfluidics based genomic microarrays, i.e., gene chips and microchannel enhanced capillary electrophoresis. In gene chips, disease specific marker complementary oligonucleotides are arrayed on the microchannel system and while, Deoxyribonucleic acid (DNA) samples isolated from a patient are passed through the system, any presence of disease specific DNA fragment can be promptly detected through chemical, fluorescence or electrical sensing means [12, 26, 27]. What microfluidics imparts here is the enhanced effective reaction rate, augmented mass transfer and low sample volume requirement (Fig. 4.1). Arraying multifarious disease specific markers together in a microfluidic based genomic microarray system, excellent parallel processing capability has been attained yielding simultaneous prognosis of several ailments. If gene chips have been able to transform the arena of DNA detection and quantitation, capillary electrophoresis [28, 29] has undoubtedly influenced separation and isolation of targeted gene specific DNA sequences. Juxtaposing them in a single platform, researchers have amazingly reduced the assay time from hours to seconds. With time, ever widening applications of microfluidic technology have also

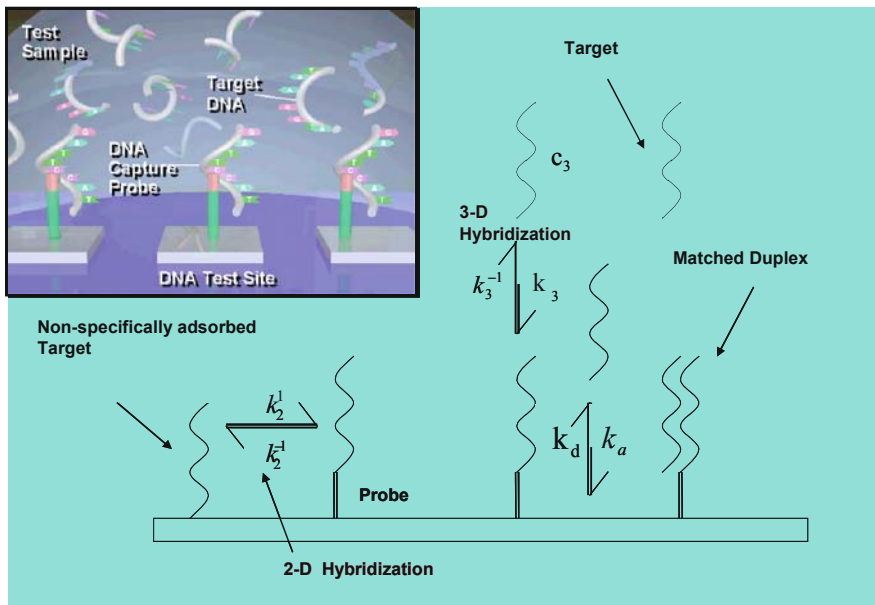


Fig. 4.1 Schematic delineation of DNA hybridization in a microfluidic platform. Surface phase (2D) hybridization in conjunction with bulk phase (3D) reaction augments the effective hybridization rate [27]

included isolation and detection of gene specific RNAs [30]. However, though capillary electrophoresis technique has been instrumental in unleashing high throughput genomics, its applications have been most prevalent in detection and separation of proteins which are physiologically important and expressed in trace level. Because of the fact that proteins of disparate functionalities may not only differ in sequence or size but also in structural conformation; separation, purification and identification of protein samples (collectively known as proteomics) are inarguably more complicated than genomic samples [31–33]. Given that a human sample contains over twenty thousand different proteins and each of them has its own characteristics isoelectric point, solubility, polarity and identifying reagents, designing a generic macro-scale proteomic assay system remains insurmountably elusive. On this very drawback, high-throughput complex biomicrofluidic systems for proteomics are emerging rapidly [34]. Microfluidic systems either performing or coupled with isotachopheresis [35], isoelectric focusing [36, 37] and mass spectrometry systems [38, 39] have become the solutions to new generation proteome biology. In another corner of proteomics, microfluidic devices have provided the most proficient solutions for protein crystallography. Three dimensional structures being uniquely deciphered from Nuclear Magnetic Resonance (NMR) and X-Ray Crystallography analysis, synthesis of protein crystal is the most indispensable stage in structural biology [40, 41]. Protocols to generate protein samples are seldom unambiguous and robust, requiring delicate control over process temperature, ionic concentration, pH and evaporation rate. Such enormity of preciseness in temporal variation of the parameters can be achieved only within microfluidic confinement.

Miniaturization and dimensional diminution in case of microchannel network have imparted most prolific effects on cell biology. Considering that biological cells dimensionally scale in the order few tens of micrometers, microfluidic platform provides an exclusive way by which they can be handled individually [10]. In some cases, on the basis of specific requirement, even different parts of a single cell can be physically or chemically manipulated through microfluidics [42–44] (Figs. 4.2 and 4.3). These functionalities have implicated utterly unfathomed niches in fundamental cell biology and associated medical diagnosis [45]. While differential addressability of diverse parts of a single cell or several neighboring cells facilitates the study of intra and intercellular signal transduction (i.e. chemical communication between different cells or different parts of a single cell) [46–50] and microfluidics based system biology [51, 52], the ability to isolate and study a single cell at a time bestows a distinctive approach to study infected cells *in vitro* [53–56]. Relevantly, on the basis of either attenuated or augmented deformability, microfluidic based detection systems pertaining to some of the lethal diseases such as cancer, malaria, AIDS and SARS have been proposed [57]. In addition, microfluidic systems, if appropriately devised, providing the closest resemblance to the physiological circulatory-renal systems and tissue matrices, confers an unparalleled platform for *in vitro* simulation of *in vivo* cellular behavior [48]. Not only that; the undeniable similitude between microchannel systems and blood vessels has encouraged researchers to adopt the technology of microfluidics in the domain of artificial tissue engineering [58]. Having explicated the need and the promising applications

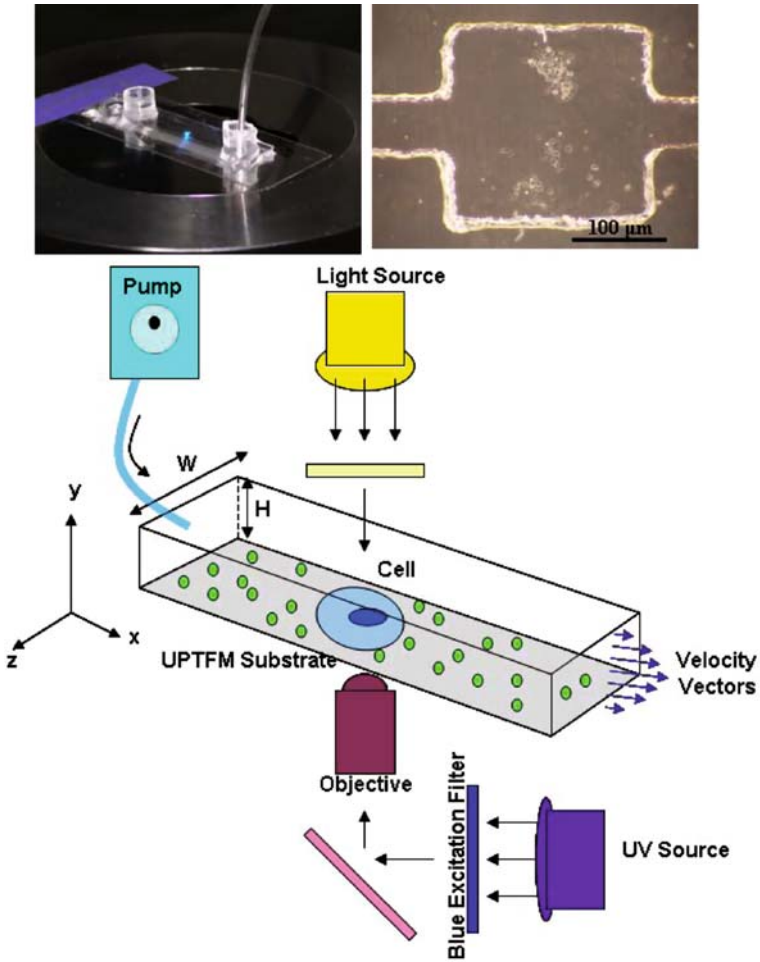


Fig. 4.2 An integrated microfluidic cell culture platform coupled with traction force microscopy [44] system. (Top Right) Square shaped microwells with adhered HeLa cells

of microfluidics technology in biological paradigm, following we discuss different physical methods and factors predominant in microfluidic species transport, with properly emphasizing relevant biological utilizations.

4.2 Diffusive Transport of Biochemical Species

Diffusive transport is intrinsic. Diffusion is the process by which a concentrated group of particles in a volume will, by Brownian motion, spread out over time so that the average concentration of particles throughout the volume is constant [59]. Under a finite temperature, diffusion arises because of the collisions between solute particles or molecules and solvent molecules. Between two successive collisions, solute

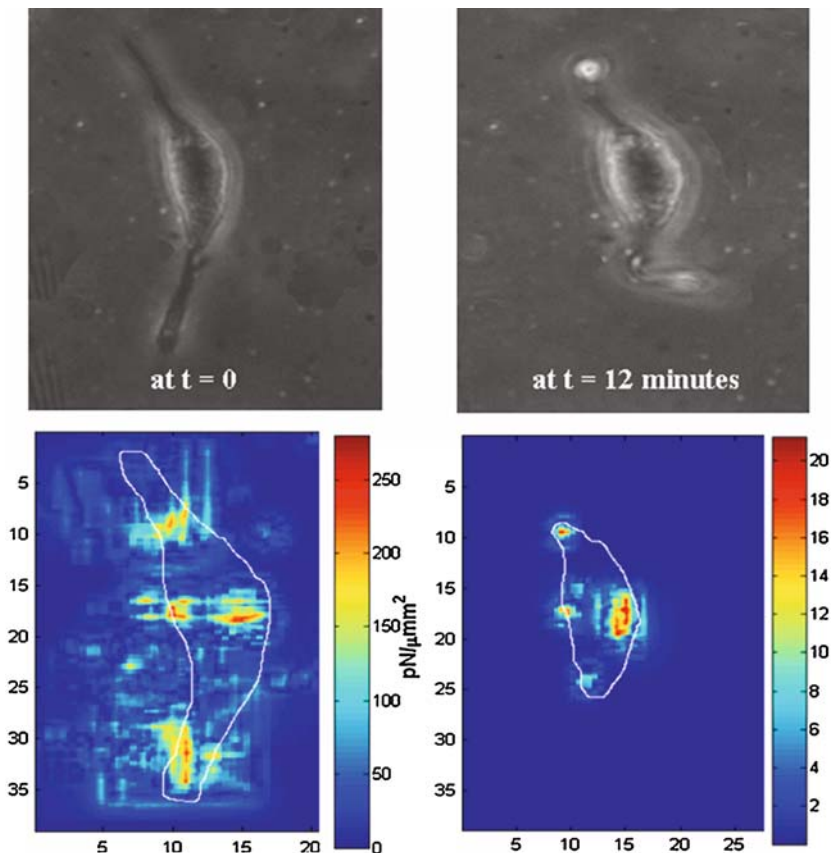


Fig. 4.3 Change in the traction force landscape as L929 mouse fibroblast cell is detached by enzymatic treatment

molecules, in this case biological macromolecules such as proteins, nucleic acids, hormones and other organic molecules, move in a straight line, ensemble average of which is called mean free path. In a collision, molecules change their velocity and direction stochastically, spreading over all around the solvent volume and homogenizing solution concentration. Mathematically, diffusive flux (J) i.e. concentration or number of molecules crossing unit surface during unit time is proportional to the gradient of concentration (∇c), with proportionality coefficient called as diffusion coefficient (D). This law is known as Fick's law and is given as follows:

$$J = -D\nabla c \quad (4.1)$$

In this equation minus sign arises out of the fact that diffusion proceeds opposite to the concentration gradient of solute molecules. The argument goes like this. If we imagine a hypothetical barrier between two volume segments of the solvent

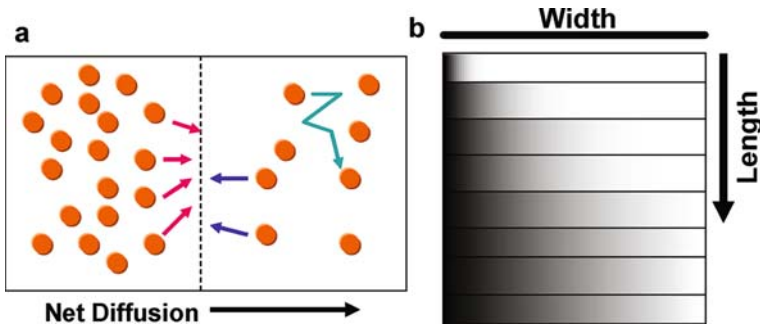


Fig. 4.4 (a) Net diffusion takes place opposite to the concentration gradient. (b) Diffusive mixing along the length of a microchannel

(Fig. 4.4), molecules from both sides should cross the barrier. However number of crossing molecules is higher from high concentration to low concentration direction than the reverse one. Thus net molecular transport occurs against the concentration gradient till the solution becomes homogeneous. The dimensionality and unit of diffusion coefficient is given as $[\text{Length}]^2/[\text{Time}]$ i.e. m^2/s respectively. Then, a generalized convection-diffusion equation is obtained by putting Fick's law into the mass balance equation, yielding

$$\frac{\partial c_i}{\partial t} + v \cdot \nabla c_i = \nabla \cdot (D \nabla c_i) + R_i \quad (4.2)$$

And in expanded form

$$\frac{\partial c_i}{\partial t} + \left(v_x \frac{\partial c_i}{\partial x} + v_y \frac{\partial c_i}{\partial y} + v_z \frac{\partial c_i}{\partial z} \right) = D \left(\frac{\partial^2 c_i}{\partial x^2} + \frac{\partial^2 c_i}{\partial y^2} + \frac{\partial^2 c_i}{\partial z^2} \right) + R_i \quad (4.3)$$

Here, c_i is the concentration of a i th biomolecular species, v_x , v_y and v_z are x, y and z components of velocity v . R_i is the reactive term of i th biomolecular species. In general, for standard biomolecular species, typical magnitudes of D range in order of 10^{-10} – 10^{-9} m^2/s . In general, approximating dilute solution, Diffusion coefficient can be evaluated as:

$$D = \frac{k_B T}{6\pi \mu R_H} \quad (4.4)$$

Where, k_B , T , μ and R_H are Boltzmann Constant, absolute temperature, solvent viscosity and hydrodynamic radius of solute molecules. For Brownian motion in dilute solution, root mean displacement is directly proportional to the time interval (Δt) during which the displacement has been studied, yielding the following relationship:

$$\langle x^2 \rangle = 6D\Delta t \quad (4.5)$$

However, in pertinence to intracellular diffusion or diffusion of molecules over biomembrane, this does not hold true for most of the studied macromolecules. There are three specific reasons namely molecular crowding, facilitated transport and diffusive inhomogeneity of solvent. Firstly, cytosol can not be approximated as dilute solution. In fact it is molecularly “crowded” to such an extraordinary extent that the diffusion is significantly damped and the molecules are consequently thought to undergo “subdiffusion” [60, 61]. In contrasting situation, intracellular propagation of specific molecules can be facilitated by molecular motors or secondary messenger. Though this is intrinsically a reactive mechanism, on the ground of coupled reaction-diffusion mass transport theory, reactive terms can be absorbed into the diffusion part, yielding a resultant augmented diffusive transport, known as “superdiffusion” [62, 63]. There is another way which is commonly believed to be a prime source for anomalous diffusion. Cytosol or biomembranes are highly heterogeneous and the heterogeneity varies in both space and time. Though, in principle, diffusion in heterogeneous medium can be modeled in the following way:

$$\begin{Bmatrix} j_x \\ j_y \\ j_z \end{Bmatrix} = - \begin{bmatrix} D_{xx} & D_{xy} & D_{xz} \\ D_{yx} & D_{yy} & D_{yz} \\ D_{zx} & D_{zy} & D_{zz} \end{bmatrix} \nabla c \quad (4.6)$$

These equations are significantly cumbersome and computationally expensive for obtaining even a numerical solution let alone any possibility of achieving an analytical expression. In the wake of such imposed problem, the diffusion equation (4.5) is empirically modified as

$$\langle x^2 \rangle = 6D_{eff} \Delta t^\alpha \quad (4.7)$$

Where D_{eff} is the effective diffusion coefficient and α is scaling exponent parameter. Sub and super diffusion is respectively defined for two regimes of α i.e. $0 \leq \alpha < 1$ and $\alpha > 1$.

While most of the problems in complete form of Eq. (4.3) are only numerically solvable, there are few idealized cases for which the relatively simple analytical solutions are attainable. One of cases we consider here is the diffusion of biomacromolecules in one-dimension (x) from a point source. The point source at $x = 0$ is mathematically modeled as

$$\begin{aligned} c(x, t = 0) &= c_0 \text{ at } x = 0 \\ &= 0 \text{ elsewhere} \end{aligned} \quad (4.8)$$

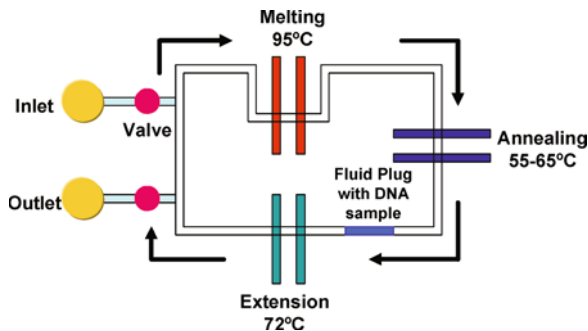
Where c_0 is initial concentration of the point source. Subsequently, $c(x, t)$ is solved as following

$$c(x, t) = \frac{c_0}{\sqrt{4\pi Dt}} e^{-\frac{x^2}{4Dt}} \quad (4.9)$$

The above equation suggests that with time, the solute front will take the shape of a progressively spread Gaussian curve with its maxima at $x = 0$. This spreading is known as band broadening and is one of the most common phenomena encountered while investigating biological species transport through microcapillary. It is important to realize that with an imposed velocity as in the case of capillary electrophoresis (CE), high performance liquid chromatography (HPLC), the shape evolution of solute band remain grossly unperturbed; only its maxima gets displaced along x-direction with time.

The effect of diffusive transport is most appreciably featured in biomicrofluidic version of Polymerase Chain Reaction (PCR) [20, 64]. This is a technique that has changed the direction and momentum of molecular biology which since 1950s has been predominantly dominated by reductionist ideology. PCR has enabled the researchers to fathom into the hitherto unexploited terrain of individual gene and their function. Note that the PCR and its variants have opened up new vistas of systems biology where interaction between many gene products (i.e. proteins) and the underlying regulation dynamics are being elucidated with enormous rapidity. PCR basically amplifies the chosen sequence portion of a nucleic acid chain (it may be chromosome or any DNA fragment). The working principle is based upon DNA polymerase's (the enzyme that copies a DNA sequence) dependency on the presence of a short nucleic fragment, called primer bound to its complement sequence segment of the genome. Granted an appropriate physicochemical environment, DNA Polymerase binds to the primer and commences its copying mechanism at that very location. In PCR, these primer sequences are strategically chosen such that only the desired stretch of nucleic acid sequence (i.e. template) is copied. Once produced, these newborn copies start acting as templates, amplifying the sequence in subsequent cycles of reaction. It is estimated that within 20–30 PCR reaction cycles, the desired sequence can be amplified as much as 10^6 times in number. Though it is quite fiddling to handle one single nucleic acid chain, one can, sure enough, work with one million identical copies of it. This is the manipulation of life's digital information at its best. Technically, single PCR cycle comprises of three major reactive substeps – denaturation, annealing and extension which mainly differs by its operating temperature. In typical PCR reaction cycle, these temperature values are 95° , $55\text{--}60^\circ$ and 72°C respectively. Hence, for successful completion of single PCR reaction, a device should be able to ramp up and down the reaction zone temperature at frequent basis with uncompromisable precision and the advent of microfluidics based PCR devices has banked upon this very constraint. It is understandable that within the purview of augmented surface area per unit volume of microfluidic confinement, heat transfer in and out of the reaction mixture must occur at faster rate than what is experienced in conventional macroscale PCR devices, reducing the whole operation time from hours to seconds. Microfluidics based PCR systems have been initially implemented as chamber stationary component [64, 65] and therefore, lacked the flexibility of controlling reaction rate. They have been eventually replaced by flow-through and thermal convection-driven microfluidic devices where reactive fluid is transported back and forth between three distinct temperature zones maintained within a monolithic platform (Fig. 4.5).

Fig. 4.5 Schematic representation of micro PCR



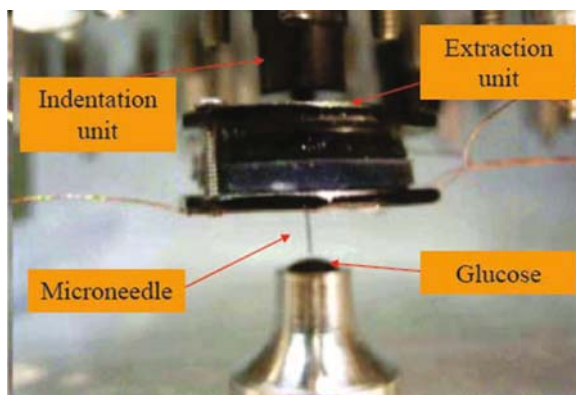
This clan of PCR systems precedes several variants such as Single straight capillary based flow-through PCR microfluidics, On-chip serpentine rectangular channel based flow-through PCR microfluidics and Circular arrangement of three temperature zones for flow-through PCR microfluidics. If it appreciated that the cycle time of PCR depend on the synthesis rate of the polymerase and subsequent diffusion time, diffusion plays a pivotal role in microfluidic PCR systems. Not only this, diffusion possesses its importance in mixing of several ingredients required for a successful PCR. Essentially these components are transported as separate entities dissolved in either similar or different buffers. Within microfluidic framework they coalesced or merged and in consequence, mixing occurs by diffusion. In absence of turbulence which is often serves as facilitator of mixing in larger scale devices, Brownian dynamics governed diffusive mixing emerges as the key player. One must note that rapid formation of a homogeneous solution is the most important step to achieve a uniform and maximum efficiency reaction. For microchannels diffusion accelerates the process.

While in macro-systems, random Brownian displacement scaling $\sqrt{6Dt}$, diffusive mixing can take intolerably long time to serve as the sole method of mixing, in microscale system the situation is quite reversed because of mainly two reasons. First, due to the reduced dimensions, characteristic time scale for diffusive propagation is comparable to the time scale of convective transport and second, diffusion requires no external power input. Being an intrinsic process which solely stems out of path of increasing entropy, it is energetically inexpensive. Hence, for natural Microsystems which has been evolving for billion years to maximizing it input versus output, diffusive mixing is an inexorable solution to mass transport problem. Most of the intracellular transport processes ferrying small molecules such as potassium, calcium ions or comparatively bigger macromolecules such as proteins, RNAs, takes the advantage of molecular diffusive transport (also know as passive transport). Only when the transport in the direction of increasing chemical concentration appears inevitable, diffusive mixing is replaced by the active processes involving consumption of intracellular energy in form of adenosine tri-phosphate (ATP) molecules. In case of extracellular transport, active processes being inaccessible, the role of diffusion becomes even more vital. One medically relevant case

is the diffusion of drug molecules through biological cell and tissues. There are three sets of governing parameters that influence drug adsorption—namely its physicochemical properties, chemical formulation and route of administration. There exist several dosage forms such as tablets, capsules and solutions which additionally include other ingredients. A specific dosage form is preferred for a particular drug which is then appropriately administered by various routes encompassing oral, sublingual, parenteral, buccal, rectal, topical and inhalational. Irrespective of the administration route, drugs should be in solution to be absorbed into the specific cell or tissue. Relevantly, drug molecules are required to cross numerous semi-permeable cell membrane barriers prior to reaching the systemic circulation. The process is executed through passive diffusion, facilitated passive diffusion, active transport, receptor mediated endocytosis or pinocytosis. Among these mechanisms, the passive diffusion is the most common and energy inexpensive manner by which the intracellular inclusion of drug molecules takes place. Drug-diffusion predominantly occurring between high to low concentration, diffusion rate is expected to be solely proportional to the concentration gradient. However, in physiological systems, effective diffusive coefficient of the drug molecules depends upon lipid solubility of drug, molecular density of extracellular space, molecular ionization and the area of absorption surface. Cell membrane being composed of lipid bilayer, diffusion of small un-ionized lipophilic drugs is favored to the highest extent. Given that the ionized molecules are weakly lipophilic, the administration route of a particular drug depends on pKa of the drug and pH of the relevant physiological fluid onto which the drug is predominantly absorbed. Hence, while for weak acids, administration through low pH medium such as gastric fluid (pH 1.5) is preferred, weak bases are principally injected directly into the blood stream (pH 7.4).

The ability to perform assays in miniaturized scale and high-throughput screening of large number of chemicals simultaneously have opened a new vistas in drug discovery and screening with microfluidics based analytical devices [66, 67]. There are several novel and upcoming spectra in this realm of application including single cell based protein isolation, analysis and ligand screening [68, 69], rapid compound generation by microfluidic combinatorial chemistry [2, 70, 71] and high-speed selection of active and pharmaceutically relevant compound. The science of microfluidics has also contributed extensively in field of drug delivery. In recent years, microfluidics-based strategies have been utilized in drug delivery devices to improve the operation time and accuracy of the process [72]. Sophisticated photolithographic procedures have been exploited to fabricate futuristic drug delivery instruments. Devices with an array of microneedles competently preserve the chemical activity of a drug compound and enable administration with characteristic cellular scale precision and most importantly, with minimal pain. Researches related to the application of microneedles (Fig. 4.6) for gene and drug delivery are essentially categorized into three broad classes namely local delivery, systemic delivery and cellular delivery [73, 74]. Microfluidics based highly localized drug delivery systems have been able to reduce the applicable doses and side effects due to non-specific drug adsorption. In addition to low molecular weight organic compounds, there are several classes of macromolecules such as proteins,

Fig. 4.6 Working principle of a microneedle which mimics the blood sampling technique of female mosquito [74]



peptides and oligonucleotides which can be successfully injected using microneedles. Performance of modern microfluidic drug delivery systems and the aptitude of sustained drug release have been significantly augmented by invoking complex fluidic circuits including a cluster of micropumps, microvalves and feedback sensors into a single microfabricated platform. Moreover, self-regulated drug delivery microdevices whose operating mechanism relies upon the biomolecular detection by “smart” polymeric compounds with interconnected feedback loops have unleashed a unique array of novel possibilities towards future advancements.

4.3 Particle Transport, Dispersion and Mixing in Biomicrofluidics

Comprehensive understanding of the local fluid dynamics in terms of the specific functional objectives of a microdevice is the key to implement a novel and effective design. In the regime of micrometer length scale where surface forces override volume forces, from the perspective of design and fabrication, the projected transport, mixing, separation and manipulation of particles hold the positions of utmost importance. One useful tool of the systemic approach is definitely the dimensional analysis. Here, one may ignore the terms where Reynolds number appear as a multiplying pre-factor after normalization. Instead, flow physics in the confined system are thought to evolve around other dimensionless parameters, representing the mutual ratio of surface, electrical, magnetic and thermal forces. In addition, in microscale flow physics, channel geometry has been noted to play an important role [75–77].

4.3.1 Dispersion

The supremacy competition between convection and diffusion is fatefully significant for many Biomicrofluidics application involving mass transport and chemical

reactions. In a pressure-driven flow, dispersion of the solute generally occurs much more elaborately than the theoretical prediction considering the sole effect of diffusion. In this case, every streamline of parabolic flow profile is browsed by solute particles due to their inherent Brownian motion [78]. The aforementioned events are analytically accounted in Taylor-Aris approach and hence, this type of dispersion is recognized as Taylor-Aris dispersion [79]. In Taylor-Aris approach it is not presumed that in advection-diffusion field, net solute transport can be explained simply by superimposing advection and diffusion. Instead, effective diffusion is appreciated to be dependent on the imposed velocity field. This occurs due to the finite transverse gradient of velocity field which becomes predominant in cased pressure-driven flow situation. For fluid carrying microparticles of concentration c through a microcapillary of radius R , the axisymmetric (x,r) advection-diffusion equation can be described as

$$\frac{\partial c}{\partial t} + u(r)\frac{\partial c}{\partial x} = D \left[\frac{\partial^2 c}{\partial x^2} + \frac{1}{r} \frac{\partial c}{\partial r} + \frac{\partial^2 c}{\partial r^2} \right] \quad (4.10)$$

where the pressure-driven velocity field is assumed to vary only in radial direction and therefore, can be approximated as

$$u(r) = 2\bar{u} \left(1 - \frac{r^2}{R^2} \right) \quad (4.11)$$

where \bar{u} is the mean velocity. Further, a no flux boundary condition should provide $\partial c / \partial r |_{r=R} = 0$ at the capillary surface. In Lagrangian coordinate system moving with average velocity of the fluid, the equation (4.10) can be rewritten as

$$\left[\frac{\partial c}{\partial t} + \bar{u} \frac{\partial c}{\partial x} \right] + \bar{u} \left(1 - \frac{2r^2}{R^2} \right) \frac{\partial c}{\partial x} = D \left[\frac{\partial^2 c}{\partial x^2} + \frac{1}{r} \frac{\partial c}{\partial r} + \frac{\partial^2 c}{\partial r^2} \right] \quad (4.12)$$

Now, in Taylor-Aris approach it is assumed that the concentration gradient along x -axis constant i.e.

$$\frac{\partial c}{\partial x} = \frac{\partial \bar{c}}{\partial x} = \text{constant} \quad (4.13)$$

where \bar{c} is average concentration over the capillary cross-section and formulated as

$$\bar{c} = \frac{1}{\pi R^2} \int_{r=0}^{r=R} c 2\pi r dr \quad (4.14)$$

It further implies that the term $D \frac{\partial^2 c}{\partial x^2}$ can be dropped from the equation (4.12). In fact for bulk of situation axial change in particle concentration has been revealed to be negligibly small in comparison to the radial change, superbly vindicating the

aforementioned approximation. Subsequently, utilizing the relation given in equation (4.13) the solution for the reduced version (i.e. $D \frac{\partial^2 c}{\partial x^2} = 0$) of Eq. (4.12) should be obtained as

$$c = \bar{c} + \frac{\bar{u}R^2}{4D} \frac{\partial \bar{c}}{\partial x} \left[\frac{r^2}{R^2} - \frac{r^4}{2R^4} - \frac{1}{3} \right] \quad (4.15)$$

after little mathematical manipulation and rearrangement. From this relation, the net flux describing the average mass flow (Q) through unit capillary cross-section is evaluated as

$$j = \frac{Q}{\pi R^2} = \frac{1}{\pi R^2} \int_{r=0}^{r=R} uc2\pi r dr = - \left(\frac{R^2 \bar{u}^2}{48D} \right) \frac{\partial \bar{c}}{\partial x} \quad (4.16)$$

comparing it with one dimension version of Fick's equation (4.1) obtained as $j = -D \frac{\partial c}{\partial x}$, one can easily notice that the effective diffusion coefficient (D_{eff}) can be analogously determined as

$$D_{eff} = \frac{R^2 \bar{u}^2}{48D} \quad (4.17)$$

It is pertinent to note that Taylor-Aris approximation is valid only when \bar{u} is sufficiently large to impose a strong velocity gradient in radial direction. When this is applicable, one may automatically expect that $D_{eff} \gg D$, implicating

$$\frac{R^2 \bar{u}^2}{48D} \gg D \text{ i.e. } \left(\frac{\bar{u}R}{D} \right) \gg 7 \text{ i.e. } Pe \gg 14 \quad (4.18)$$

Here, Pe is the Peclet number $\left(\frac{2\bar{u}R}{D} \right)$ which represents the relative strength of convective and diffusive transport. Thus, in the regime of convective-diffusive transport through microchannel Peclet number is major non-dimensional number.

For the applications where dispersion is undesired as in solution purification and isolation, electrokinetic strategy performs superior than pressure driven mechanism owing to its innate uniform velocity profile across the channel width. However, a caveat must be sounded that in nanochannel or in very dilute ionic medium where electric double layers formed due to the surface charges overlap, even electrokinetic flow becomes parabolic yielding significant dispersion. Also the residence time of solute molecules inside the intended zone becomes a governing factor and in reduced time scale, suspended solute particles may not diffusively encompass the entire channel. It leaves Taylor-Aris dispersion analysis invalid in this case and the effectual chemical reactions are controlled by the local velocity profiles within microchannel. This generally generates an increased band broadening towards the microchannel center.

4.3.2 *Mixing*

It is important to note that characteristics biomolecular diffusion coefficients are of the order of 10^{-10} m²/s. Hence, for a microchannel with 10 μm width and 1 mm/s average flow velocity, approximately 100 channel widths i.e. 1 mm length is required for the completion of mixing solely by diffusion. In order to circumvent such low-strength diffusive mixing, different inventive strategies targeting mixing by incipient transverse flow have been designed. Further, forced mixing becomes inevitable at small scales because of the macroscale-specific turbulence dependent mixing is no more accessible. In biomicrofluidic systems, mixing is achieved either by passive mechanisms [80] such as Hydrodynamic focusing, flow separation, flow split-recombination and chaotic advection. It appears spontaneously rational that augmenting the mixing of a tracer in a fluid or two fluids will be facilitated considerably by chaotic advection mechanism [81]. The essential principle of chaotic mixing is the generation of secondary flow or transverse flow patterns exploiting the action of either centrifugal forces in curved channels or purposefully patterned microchannel surfaces. In order to produce chaotic flow profiles, stream lines should cross each other at different times. Again, according to the theory of dynamic systems, in two dimension (2D), chaotic particle motion arises only in cases with time-variant velocity field. In three dimensional flow, however, chaotic motion may be observed for even time-invariant velocity field. The incidence of chaotic advection intrinsically facilitates fast distortion and elongation of fluid elements, thereby increasing the two-fluid interfacial area across which diffusion takes place. The most prominent advantage with passive mixing such as chaotic advection is the ability to be operational without requiring external energy input. However, the passive mixing process being ingrained within the architecture of the microchannel network, it is not controllable in spatio-temporal scale. Here, one may have to invoke active mixing strategies. Active micromixing depends on applications of external energy which induces disturbance in the flow fields. In active mixing, transverse flow is generated by using either hydrodynamic or electrokinetic approaches. Approaches that have been previously employed to enhance mixing performance in active format include piezoelectrics, pneumatics, acoustics, electroosmosis, dielectrophoresis, magnatohydrodynamics, electrowetting of droplets and time dependent generation of transverse flow. Among the aforementioned strategies, variations of zeta potential at the channel wall have been the most promising protocol [82]. Alternative spatial patterns of induced zeta potential create a microcirculation within the flow field, which in turn catalyses the mixing process (Fig. 4.7).

4.3.3 *Separation Processes*

Separation of different kinds of biomolecules of varying in size molecular weight, chemical composition or even optical isometry stays at the epicenter of analytical biochemistry. In microfluidics, for effective and fast separation of

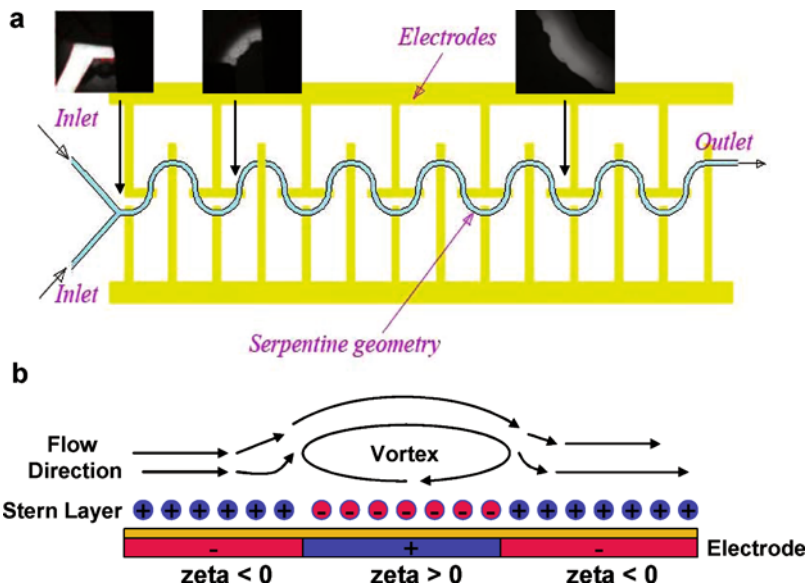


Fig. 4.7 Combined active-passive micromixing in a serpentine microchannel with alternatively charged embedded electrodes

biomolecules, electric and thermal cross fields are generally employed to achieve augmented spreading of an injected solute in the flow direction. Other methods for separation and enhancement include surface modification, hydrodynamic interaction and micro-nano sized post array for preferentially hindered motion of solute particles.

Field-Flow Fractionation (FFF) is defined as the broad clan of separation methodologies where solute zones are primarily layered at the side of a microchannel by the appliance of external field [83]. Interaction between field and solute governs the layer thickness (Fig. 4.8). Subsequently, longitudinal flow mediated displacement of solute layer takes place. Since in a typical pressure driven flow, flow velocity decreases away from the channel center, the displacement solute layers is differentially retarded depending upon their proximity to channel wall. Hitherto used perpendicular fields include Thermal gradients (Thermal FFF), electric field (Electrical FFF), magnetic field (Magnetic FFF), electrothermal gradient (Electrothermal FFF) [84] and centrifugal forces (Sedimentation FFF). The applicability of each of the aforementioned FFF technologies is guided by the potency and specificity of field-solute interaction. Owing to field-solute interaction, solute is transported in transverse direction with a velocity u_T . In steady state condition, diffusion acts in the reverse direction, along the negative u_T axis and the formed layer possesses characteristic thickness l given by the relation $l = D/|u_T|$.

In functional applications, FFF has startling similarity with chromatography yet it encompasses a broader range of solute purification with enhanced resolution,

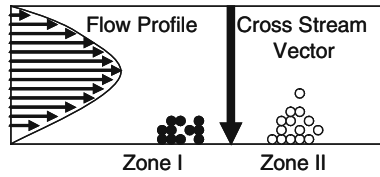


Fig. 4.8 Schematic representation of field flow fractionation. Cross stream vectors are created by electro, thermal, electro-thermal, magnetic mechanisms

augmented process rapidity, easy operation and interface with other sensor-detecting device. With relevance to Biomicrofluidics [85], Hyperlayer mode FFF (HyFFF) is the most important technique [86] belonging to FFF class with its capability separate a wide range of particles with variable diameters (0.5–50 μm). In this mode of methodology, particles are transported by the shear force or hydrodynamic lift force yielding faster dilution of larger particles than the smaller ones.

The Electric field mediated FFF (EFFF) relies upon application of an electric field in the transverse direction with respect to flow [87]. In tune with the underlining working principle of FFF technology, EFFF works by forcing the particles towards different locations between microchannel center and the solid wall. The localization of particles is governed by their intrinsic electrophoretic mobility or surface charge with highly mobile or highly charged particles moving in proximity of the solid wall while relatively uncharged particles form a diffused cloud close microchannel center. The displacement of particles toward the channel being counteracted by diffusive effects, equilibrium average thickness of the particle layers is obtained from a magnitude balance between diffusive and electric forces. Owing to the parabolic profile of the longitudinal velocity field, particles staying close channel center are moved further than the particles layering close to the channel wall. Evidently, in this method particles are separated on the basis of their electrophoretic mobility or zeta-potential which are pivotal parameters deciding a particle's transport across cell membrane, hormonal control and antigen-antibody interaction. EFFF has been applied to separations cells, large molecules, colloids, emulsions and delicate macromolecular compounds such as liposomes for which electrophoretic separation had been infeasible method.

In Thermal gradient mediated FFF (TFFF) system [88], the solute particles are differentially layered with application of spatially varying temperature field across the channel width. Here, particles are segregated depending upon their relative thermal diffusophoretic mobility or thermal diffusion coefficient (D_T). As in EFFF, the particles having higher D_T layers close to channel wall and in consequence, their longitudinal motion is highly impeded. The disparity in average velocity influences the spatio-temporal separation of the sample solute components at the output side of the TFFF channel. Thermal field-flow fractionation (TFFF) has generally been utilized in polymer separation, purification, and analysis.

4.4 Biochemical Reactions in Bio-Chips

4.4.1 General Reaction Scheme

For a generalized reaction of the form:



The rate of the reaction can be given as

$$\begin{aligned} r &= \frac{1}{d}r_D \left(= \frac{1}{d} \frac{d[D]}{dt} \right) = \frac{1}{c}r_C \left(= \frac{1}{c} \frac{d[C]}{dt} \right) \\ &= \frac{1}{a}r_A \left(= -\frac{1}{a} \frac{d[A]}{dt} \right) = \frac{1}{b}r_B \left(= -\frac{1}{b} \frac{d[B]}{dt} \right) \end{aligned} \quad (4.20)$$

Further, given that for most of the cases, it is indispensable to determine the kinetics of a reaction from known parameters such change the is concentration of a particular component, the rate of the reaction can be expressed as

$$r = k[A]^{a_1}[B]^{b_1} \quad (4.21)$$

k is the rate constant and a_1 and b_1 are the coefficients which may or may not be equal to (a, b) . Subsequently, the order of reaction is defined as

$$n = a_1 + b_1 \quad (4.22)$$

Evidently the unit of rate constant is dependent on n and is expressed as $[mol/m^3]^{1-n}/s$ i.e. for zero order reaction it is mole/m³/s; for first order reaction s⁻¹.

The rate constant strongly depends upon the Temperature of the reaction and this dependence is analytically expressed by Arrhenius equation

$$k = A_r e^{-E_a/RT} \quad (4.23)$$

Here E_a is the activation energy which is generally obtained from the difference between energy states of the reactants and the products. A_r is the Arrhenius frequency factor and represents the rate of collisions in the reactive mixture. Though for bulk of the reactions, obtaining the temporal variation in reactant concentration (as determined by analytical integration of rate equation) is impossible, it can be solved for unimolecular reaction of following type

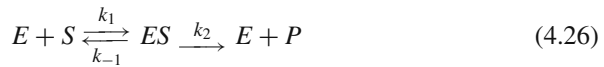


In this case, the generalized expression for a first order reaction is evaluated as

$$[A] = [A]_0 e^{-kt} \quad (4.25)$$

4.4.2 Michaelis-Menten Kinetics

Michaelis-Menten Kinetics represents a wide variety of biochemical reactions including enzyme-substrate interaction, antigen-antibody binding, DNA hybridization, protein-protein interaction and many more. Following, for sake of simplicity we describe the kinetics for enzyme-substrate interaction while other should follow similar methodology of formulation. In the beginning, it is formalized that an enzyme E which is a biochemical catalyst, acts upon a chemical species S (i.e. Substrate) to get the later converted into the product P. In the process, E is transiently associated with S forming a complex ES which is consequently converts into the product and the unchanged enzyme E again. The scheme is represented as



Assuming, rate constant are given as k_1 , k_{-1} and k_2 , the change in the concentration of complex ES can be summarized as

$$\frac{d[ES]}{dt} = k_1[E][S] - k_{-1}[ES] - k_2[ES] \quad (4.27)$$

Michaelis-Menten scheme presumes that ES achieves a steady state under its rapid conversion to P. Using this approximation, Eq. (4.27) can be rewritten as

$$\frac{d[ES]}{dt} = k_1[E][S] - k_{-1}[ES] - k_2[ES] = 0 \quad (4.28)$$

Which can be manipulated further to

$$[E][S] = \frac{k_2 + k_{-1}}{k_1}[ES] \quad (4.29)$$

$$\text{Or } [ES] = \frac{k_1[E][S]}{k_{-1} + k_2} = \frac{[E][S]}{K_m} \quad (4.29a)$$

K_m is the Michaelis-Menten constant and represents the enzyme-substrate affinity in an inverse sense. Further, expressing total enzyme concentration $[E_0]$ as

$$[E_0] = [E] + [ES] \quad (4.30)$$

We obtain

$$[ES] = \frac{([E_0] - [ES])[S]}{K_m} \quad (4.31)$$

Or identically

$$[ES] = \frac{[E_0][S]}{K_m + [S]} \quad (4.31a)$$

Given that the velocity of the reaction is expressed as

$$v = \frac{d[P]}{dt} = k_2[ES] \quad (4.32)$$

The final Michealis-Menten kinetic equation is given as

$$v = k_2[ES] = \frac{k_2[E_0][S]}{K_m + [S]} = \frac{v_{\max}[S]}{K_m + [S]} \quad (4.33)$$

Here, v_{\max} is the maximum velocity of the reaction and is assumed as $k_2[E_0]$. Michealis-Menten relation can be expressed in another alternative form, famously recognized Lineweaver-Burk expression

$$\frac{1}{v} = \frac{1}{v_{\max}} + \frac{K_m}{v_{\max}} \frac{1}{[S]} \quad (4.34)$$

It should be noticed from Eq. (4.34), that if $1/v$ is plotted against $1/[S]$, the intercept and the slope are given as $1/v_{\max}$ and K_m/v_{\max} respectively.

One of the recognized utilities of Lineweaver-Burk expression is its ability to delineate the nature of inhibition. It is known that while the reactions allowing competitive inhibition alter the x-intercept value, maintaining the magnitude of y-intercept, noncompetitive inhibitory reactions do the reverse.

4.4.3 *Langmuir Adsorption Model*

Similar to Michealis-Menten model which characterizes a representative biochemical reaction, the adsorption of a biomolecular species is, in general, is simulated by Langmuir model. In this model, the sample case is considered as the adsorption of a biomolecule from a solution onto a solid surface and the reverse desorption process. If we denote the molecules in solution and surface-adsorbed phase by S and Ω , then the process is given as:



If the maximum concentration of the surface-adsorbed molecule is assumed as Ω_0 , the net rate of adsorption can be written as

$$\frac{d\Omega}{dt} = k_a[S]_w(\Omega_0 - \Omega) - k_d\Omega \quad (4.36)$$

$[S]_w$ is the concentration of S at the solid surface or wall as in case of a microfluidic system. The Eq. (4.36) can be integrated in time to delineate the evolution of Ω

$$\Omega(t) = \frac{k_a[S]_w\Omega_0}{k_a[S]_w + k_d} \left(1 - e^{-(k_a[S]_w + k_d)t}\right) \quad (4.37)$$

which asymptotically reaches to a value of $\Omega = \frac{k_a[S]_w\Omega_0}{k_a[S]_w + k_d}$ as $t \rightarrow \infty$. Whereas for small time, Ω takes a much simpler form of

$$\Omega = k_a[S]_w\Omega_0 t \quad (4.38)$$

Though Michaelis-Menten kinetics and langmuir models are suitable approximations, for general biochemical reaction occurring in microfluidic system, the appropriate contribution of fluid flow should be appreciated. The system then becomes an advection-diffusion-reaction system which modeled in similitude to Eq. (4.2) with the reactive term R_i obtained from the underlining rate law. For example if we consider a simple reaction of type $mA + nB \rightarrow pC$ with reaction rate k , the mass transport equations for three chemical become

$$\frac{\partial c_A}{\partial t} + v \cdot \nabla c_A = \nabla \cdot (D_A \nabla c_A) - mk_{ACB} \quad (4.39a)$$

$$\frac{\partial c_B}{\partial t} + v \cdot \nabla c_B = \nabla \cdot (D_B \nabla c_B) - nk_{ACB} \quad (4.39b)$$

$$\frac{\partial c_C}{\partial t} + v \cdot \nabla c_C = \nabla \cdot (D_C \nabla c_C) + pk_{ACB} \quad (4.39c)$$

which under simplified and reduced condition may behave like a Lotka-Volterra system.

Microfluidics systems have revolutionized the field of enzyme kinetics, particularly inhibition kinetics, because they require low volume of analytes and allow unprecedentedly rapid output generation [89, 90]. Microfluidic assay systems are grouped into two main broad categories namely offline and online inhibition studies. Online inhibition studies can further be divided into homogeneous and heterogeneous reactive systems. In offline inhibition studies, reaction is performed separately in macroscale and after a scheduled time, a sample volume is withdrawn, which is then separated and analyzed using microfluidics based capillary electrophoresis method. For example, offline enzyme inhibition assays have executed to investigate inhibition kinetics of several biologically relevant enzymes including β -glucuronidase [91, 92], β -galactosidase, protein kinase A [93] and src kinase [90]. These systems seemingly offer two major advantages. Firstly, microfluidic based CE increases the efficiency and the resolution of component separation-identification and secondly, it eases a very low sample volume requirement. However, being predominantly operated in macroscale, the offline assay systems fail to savor the complete package of microfluidic advantages and in order to eliminate this

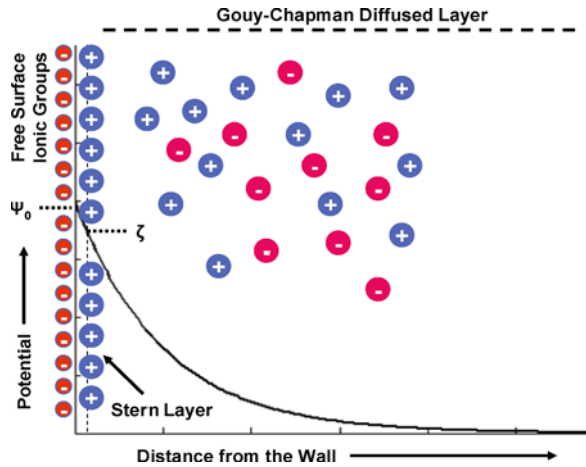
drawback; online enzyme assay devices have been implemented, which critically juxtapose both reaction and separation processes in a monolithic microchannel network system. In an online assay system, one of its components may be immobilized into the solid microchannel wall or all of them may be dissolved into the fluid phase. They are known as heterogeneous and homogeneous inhibition assay systems respectively [90]. While the heterogeneous type offers ultra-low component (enzyme, substrate or inhibitor) volume constraint and higher controllability of spatiotemporal reaction dynamics, the process is often restricted by the spontaneous partial or complete inactivation of a chemical component undergoing immobilization. The system requirement varying case to case, apparently, both of them have found their application niches. The list of enzymes studied under the heterogeneous system includes uridine diphosphate glucuronosyltransferase, angiotensin converting enzyme, HIV protease and β -galactosidase. Concurrently, inhibition kinetics of adenosine deaminase, acetylcholinesterase, liver rhodanase have been scrutinized using homogeneous biochip based inhibition assay methods [90].

4.5 Bio-Micromanipulation Using Electrical Fields

The electroosmotic flow arises when bulk fluid motion is powered by the stresses concentrated in charged layers near charged wall interface [94, 95]. The resulting velocity profile becomes uniform between channel walls except for very thin region near the interface. This kind of situation occurs when a charged surface is exposed to an ionic fluid. Owing to the strong attractive interaction of coulombic nature, counter ions migrate towards the charged wall and thereby, form an approximately immobilized ion layer called Stern layer. Subsequently, over this immobilized layer, a diffused layer of solubilized ions is created due to the counter-active effect of coulombic interaction and forces derived out of the entropic contribution. This segment is called the Gouy-Chapman layer (Fig. 4.9). Once an electric field is externally applied on the system, charged double layer acquires a velocity towards a definite electrode depending upon the net polarity of the wall charges. For electroosmotic flow, the velocity scales linearly with the electric field. Similar scaling relationship is also obtained for electrophoresis where charged particles moves under the direct interaction with imposed electric field and in turn, they drag the hydration layer formed around them. In contrast, for dielectrophoretic phenomena where movement originates essentially because an electrical dipole interacts with the gradient of the electric field, the response is deduced to be proportional to the square of the electric field.

From the very origin of microfluidics, electrokinetic methods have widely appreciated as the most suitable flow driving, actuation and component separation mechanism for several biologically relevant devices such as capillary gel electrophoresis, microchannel based liquid chromatography system and particle concentrator. In general, electrokinetic mechanisms are preferable because of several reasons enlisted below. First, for a microchannel of height h and width w , for

Fig. 4.9 Schematic representation of electric double layer formation at charged microchannel surface



a fixed potential difference, electroosmotic flow rate appears to be proportional to $h \times w$ which stands in contrast to pressure driven flow where volumetric flow rate is proportional to $h^3 \times w$. Second, diminished cross sectional area of microfluidic architecture enforces enhanced electrical resistance to ionic currents, which guarantees high electrical fields (>100 V/cm) to be persisted with low currents. Third, in small systems, thermal convection opposing the electrokinetic motion is appreciably prevented due to viscous damping. Lastly, for channels without significant design and compositional heterogeneity, the electroosmotic plug flow facilitates uniform transport of biological samples effectively eliminating any band broadening due to hydrodynamic dispersion.

In order to achieve efficient momentum and energy transfer for controlling the motion of fluids and molecules, it is important to have operational length-scale matching in an approximate scale. Pertinently, bulk of the biological entities of interest, such as DNA, proteins, and cells, have a characteristic length from nanometer to micrometer. Electrokinetics transport and flow actuation mechanisms are especially effective in this micron and sub-micron regime as they advantageously utilize the inherent small length scale. In addition, with the progress of micro-electromechanical systems (MEMS) fabrication technology, integration of micro or nano scale electrodes to polymer based fluidic device has become a trivial procedure. These effects, in combination, make electrokinetic forces ideal for manipulation and control of biological objects and performing desired fluidic operations. By utilizing electrokinetic effects, fluid flow can be manipulated, in general, using the electro-osmosis, AC electro-osmosis, electrophoresis, dielectrophoresis, electrowetting and electrothermal phenomena.

Before we proceed to describe each of aforementioned events in detail, evidently, as it becomes essential to comprehend the physical mechanism undergoing beneath the formation of Debye layer, before going to sub-categories of electric field based

methods, we present an abridged formulation illustrating the counter ion distribution around a charged colloidal particle. From the Poisson equation describing the relation between the charge density ρ and potential ψ , it is known that

$$\nabla^2 \psi = -\frac{\rho}{\varepsilon_0 \varepsilon_r} \quad (4.40)$$

Where ε_0 and ε_r are vacuum and relative permittivity respectively. From this equation, in order to determine ψ , one must possess the knowledge of ρ at hand, which, in turn, should be available from the number densities of relevant ionic specie (n_i), as given by Boltzmann distribution

$$n_i = n_{i,0} \exp[-z_i e \psi / k_B T] \quad (4.41)$$

Here, z_i , $n_{i,0}$, e and k_B are ionic valency of i th species, ion concentration at bulk, elementary electronic charge and Boltzmann constant respectively. For symmetric electrolytes (e.g. NaCl, CaSO₄ etc.) net charge density is given as

$$\rho = n_0 [z e \exp(z e \psi / k_B T) - z e \exp(-z e \psi / k_B T)] \quad (4.42)$$

i.e.

$$\rho = n_0 z e [\exp(z e \psi / k_B T) - \exp(-z e \psi / k_B T)] \quad (4.42a)$$

Theoretically putting the expression (4.42a) in (4.40) the variation in ψ can be solved. However, one may easily notice that, in this process, analytical solution is impossible to deduce. Hence it is further approximated that thermal energy is much higher than electric energy implying $k_B T \gg e \psi$. Under this assumption which is known as Debye-Hückel approximation, the Eq. (4.42a) can be linearized yielding an one-dimensional expression

$$\psi = \psi_0 \exp(-\kappa x) \quad (4.43)$$

Where ψ_0 is the potential at surface and κ^{-1} is the Debye length deduced as

$$\kappa^2 = 2 \frac{z^2 e^2 n_0}{\varepsilon_0 \varepsilon_r k_B T} \quad (4.44)$$

Evidently from Eq. (4.44), Debye length inversely depends upon the salt concentration. Typical value of Debye length lies in range of few nanometers for moderate concentrated salt solutions (100 mM) which are commonly used in biochemical experimentations.

4.5.1 Electroosmosis

Electroosmosis arises due to the development of electrical double layer at charged surfaces. When an ionic liquid is brought in contact with a charged solid surface, the surface charge is neutralized by counter ions in the ionic medium. The immediately layer of counter-ions which is approximated to immobilized is called Stern Layer. Beyond this immobilized and exclusive region of counter ions, there exists an outer region, where ions are in rapid thermal motion, and the layer is known as the diffuse electrical double layer (EDL) that spans a distance on the order of the Debye length (Gouy-Chapman Layer). An illustrative depiction of the aforementioned phenomenon has been given Fig. 4.9. Now, if an electric potential is externally applied along the channel, the diffused electrical double layer starts moving owing to the net electrostatic force. As the ions in the EDL move, they drag water molecules along themselves due to the cohesive nature of the hydrogen bonding of water molecules. The entire event then yields to a net movement of buffer solution. For an electroosmotic flow field, the reduced Navier-Stokes equation (neglecting convective and pressure terms) can be written as

$$\rho E + \mu \frac{\partial^2 v}{\partial z^2} = 0 \quad (4.45)$$

Where E is the applied electric field. The charge density can be obtained from Poisson Eq. (4.40) as

$$\rho = -\varepsilon_0 \varepsilon_r \nabla^2 \psi \quad (4.46)$$

Combining (4.45) and (4.46) we obtain

$$E \varepsilon_0 \varepsilon_r \frac{\partial^2 \psi}{\partial z^2} = \mu \frac{\partial^2 v}{\partial z^2} \quad (4.47)$$

And with the following boundary conditions

$$\begin{aligned} v|_{wall} &= 0 \\ \psi|_{wall} &= \zeta \\ \partial \psi / \partial z|_{bulk} &= \partial v / \partial z|_{bulk} = 0 \end{aligned} \quad (4.48)$$

The final expression for v yields

$$v(z) = \frac{\varepsilon_0 \varepsilon_r E}{\mu} [\psi(z) - \zeta] \quad (4.49)$$

As the potential exponentially decreases away from the wall surface, the electroosmotic velocity at the bulk can be deduced as

$$v_{eo} = -\frac{\varepsilon_0 \varepsilon_r E \zeta}{\mu} \quad (4.50)$$

From the deduction furnished above, it is evident than for electroosmotic flow, velocity remains constant across the channel width reducing the magnitude of sample dispersion. This stands in contrast to highly dispersive pressure driven flow where velocity profile assumes a parabolic shape with a maximum at channel center line. In order to capitalize this benefit in microfluidic regime, electroosmotic flow has been recurrently used for sample injection in electrophoresis-based separation devices. In a generic design of such device, silica particles are packed in a fused silica capillary and the porous glass structure enables a high surface-to-volume ratio, augmenting the electroosmotic effect. Further, if the separation between bounding wall surfaces becomes commensurate to the Debye length, the effect of the electrical double layer overlap in governing the flow profile should be accounted [96]. Typically, glass substrates are utilized due to their well-investigated surface properties and surface modification techniques by chemical means. However, in tune with advancements of polymer-based microchannel systems, recently, the procedure has also been demonstrated in some appropriate polymeric materials such as Polydimethylsiloxane (PDMS), Polymethylmethacrylate (PMMA) and Polystyrene. One plus point of these materials is that they can be easily molded into complex network architecture, required in many microfluidic high-throughput assay systems. With application of polymeric materials possessing chemically or physically tunable surface potential properties, electroosmotic pumping has been demonstrated in complex networks of intersecting capillaries where the fluid flow can be controlled quantitatively by simultaneously applying potentials at several judiciously chosen locations [97]. However, the flow actuation through complex fluidic surface frequently imposes challenging situations from an analytical point-of-view. Fortunately, the electroosmotic flow being directly connected to the electric current, it can be trivially estimated by considering the equivalent resistive circuit and electroosmotic mobility in analogy to the well-established current analysis in electric circuits. Here it is to be appreciated, electroosmotic flow gifts us with another control in the form of surface potential which can be dynamically manipulated either by chemical treatment or by transverse electric field. A perpendicular electric field has been illustrated to alter the zeta potential. In conjunction, spatial modifications of electroosmotic mobility have been reported with protein adsorption and viscous polymer channel sidewall coatings. The situation becomes non-trivially interesting when one uses patterned surface charges. In fact, bi-directional electroosmotic flow and out-of-plane vortices have been demonstrated with different surface charge patterns [98]. The capability of generating flow patterns offers the potential for achieving microscale mixing with enhanced efficiency.

4.5.2 AC Electroosmosis

AC electroosmosis is a recently identified electrokinetic phenomenon observed at frequency ranges below 1 MHz [99–101]. This observation has been reported for aggregation of yeast cells in interdigitated castellated electrodes. Though

different in the nature of applied electric field, AC and DC electroosmosis possess an impending original similitude in mechanistic principle that they both exert a tangential force on electric double layer. Electric potential within the electrode forces the charges to build up concentration on the electrode surface. Subsequently the interfacial charge density is altered and formation of the electrical double layer takes place. The process is known as electrode polarization. The electrical double layer, now, experiences a net force due to the tangential component of the electric field and result in fluid movement. In alternating electric field, the sign of charges in the electrical double layer periodically oscillates with the oscillation of applied electric field and therefore, its tangential component. Therefore, the direction of the driving force for the fluid remains unaltered.

4.5.3 Electrophoresis

Electrophoresis describes the movement of charged particles in a liquid medium under an external electric field. When a particle with charge q is under a steady electric field E , the particle experiences an electrostatic force qE . The electrical force is balanced by a friction force, which can be estimated by Stoke's law, $6\pi\mu Rv$ for a spherical object. Velocity of the particle can be related to the applied field by the relation

$$V = \mu_{eph}E \quad (4.51)$$

Where μ_{eph} is the electrophoretic mobility. For particle with radius a and charge q_p , μ_{eph} is obtained as

$$\mu_{eph} = \frac{q_p}{4\pi\mu\kappa a^2} \quad (4.52)$$

Which is reduced to $\mu_{eph} = q_p/6\pi\mu a$ for cases with $\kappa a \ll 1$.

To cite the most relevant biomicrofluidic applications of electrophoresis, it is pertinent to mention that charged biomolecules such DNA, RNA, proteins migrate under the control of an externally applied electric field. In free solution electrophoresis, a DNA molecule adopts a structure of free draining coil, which implies that the friction coefficient remain proportional to the length of the molecule. Simultaneously, it is important to note that the net charge and therefore, the force experienced by a DNA molecule is also proportional to the length. As a result, the effective mobility of the molecules, which is basically the ratio between the externally applied force and the friction coefficient, remains independent of molecular length at a given medium condition for large DNA molecules. However, the net charge of a DNA molecule is accessible only in reduced magnitude as a fraction of the molecular charge is counter-acted and neutralized by the counterions (as determined by counterion condensation theory). For small DNA molecules, typically containing 20–100 base pairs, it is envisioned that the length dependence of

small DNA molecules arises due to the imposing consequence of counterion relaxation phenomenon. For protein or peptide molecules, the situation is not as simple as in electrophoresis of DNA. These molecules may be positively or negatively charged depending on the zwitter-ionic nature of amino acid side chains, the pH of the medium and non-intuitively, the secondary or tertiary structure of the protein. Amine side chains are predominantly exist in protonated form to give a positive charge at low pH (<5). In contrast, at high pH, carboxylic acid side chains are de-protonated to result in a net negative charge. The net charge of the protein at any pH is obtained depending upon the relative abundance of protonated and de-protonated forms of side groups. At a particular pH, characteristics of a particular protein or peptide molecule, the net manifested charge of the molecule may be nullified. This is known as isoelectric point (pI). As a result, proteins can be separated according to their mobility as well as isoelectric point, implicating a two-dimensional and high resolution separation system. In modern biological analysis which includes molecular fragment separation, sequencing and structural analysis, 2D gel electrophoresis and capillary electrophoresis with an array of separating channels, have become precious tools. Another method which takes advantage of signature isoelectric point for a specific protein or peptide is Isoelectric focusing. Here, in developed gradient of pH between two electrodes, protein molecules preferentially accumulate in their respective isoelectric point. It has been demonstrated that generation of a pH gradient by electrolysis-driven production of H^+ and OH^- ions in a microfluidic device can be utilized in separating different components from mixture of proteins and peptides [102].

4.5.4 Dielectrophoresis

Subjected to an electric field, a dipole is induced in a polarizable particle. In a spatially diverging electric field, depending upon the sign of the polarizability difference between the particle and the bulk medium, it moves towards either towards or away from the increasing electric field. This electrokinetic phenomenon is known as dielectrophoresis (DEP) [103–105]. The dielectrophoretic force on a particle with radius a and relative permittivity $\epsilon_{r,p}$ suspended in liquid with relative permittivity $\epsilon_{r,l}$ can be expressed as

$$F = 2\pi a^3 \epsilon_0 \epsilon_{r,l} \text{Re}(f_{CM}) |\nabla E|^2 \quad (4.53)$$

Where f_{CM} is the Clausius-Mossoti factor and is given by

$$f_{CM} = \frac{\epsilon_p^* - \epsilon_l^*}{\epsilon_p^* + \epsilon_l^*} \quad (4.54)$$

ϵ_p^* and ϵ_l^* are complex permittivities of particle and solvent and are formulated as

$$\varepsilon_p^* = \varepsilon_0 \varepsilon_{r,p} - j \frac{\sigma}{\omega} \quad (4.55a)$$

$$\varepsilon_l^* = \varepsilon_0 \varepsilon_{r,l} - j \frac{\sigma}{\omega} \quad (4.55b)$$

σ and ω being conductivity and frequency of the electric field.

As evident from Eqs. (4.53), (4.54) and (4.55), positive (\negative) dielectrophoresis i.e. the movement towards (\away from) the high field strength region occurs if the polarizability of bulk medium is lower (\higher) than that of the particle. DEP is commonly applicable for enforcing translational motions of different biological micro-objects. Using dielectrophoresis, different types of cells with distinct polarizabilities can be conveniently segregated. For example, it has been confirmed that a mixture of major leukocyte subpopulations, isolated from human blood sample, can be competently separated by dielectrophoresis. DEP has also been illustrated for maneuvering micron-sized biological entities such as DNA, proteins, bacteria and viruses. For small molecules, the ratio of dielectrophoretic and thermal forces governs the effective particle dynamics.

4.5.5 Electrowetting

An alternative of driving bulk fluid motion through a microchannel network is to employ droplet based digital microfluidics. Such digital fluidic system confers the performance of biological assays with minimum possible volume requirement. The droplet translation mechanism in a digital microfluidic circuit takes advantage of several physical effects such as thermocapillaries, dielectrophoresis and voltage or light mediated surface wetting, of which electrowetting on dielectric (EWOD) has been applied most abundantly due to its convenience of application, compatibility towards on-chip integration, inherent process reversibility and low power consumption. In this process, a thin dielectric film (typically, polymer materials or silicon oxide) is coated over the microfabricated electrodes in order to nullify the direct electrochemical contact-interaction between the fluid and the electrode. However, this compels the use of high voltage. If the permittivity and layer thickness of the dielectric thin film are given as ε_d and d respectively, the contact angle of liquid droplet having liquid-vapor surface tension γ_g changes from its initial value θ_0 with applied potential V , obeying the following mathematical expression

$$\cos \theta = \cos \theta_0 + \frac{1}{2} \frac{\varepsilon_0 \varepsilon_d}{\gamma_g d} V^2 \quad (4.56)$$

By the application of spatially patterned electric field, different contact angles may be invoked in different parts of a single droplet which in turn, results in net droplet motion. Since its introduction, several designs have been realized for efficient driving droplets on a two-dimensional space [106, 107].

4.5.6 Electrothermal Flow

Electrothermal flow arises because of the temperature gradient in the medium which in turn, may be generated by joule heating of the fluid [108–111]. When such temperature gradient exists within liquid medium; the conductivity, viscosity, density and permittivity of the fluid varies spatiotemporally, exerting a net mobilization force on the fluid. By judiciously designing the heating elements and electrodes, electrothermally actuated micropumps can be fabricated. These pumps eliminate the requirement for moving parts. Electrothermal effects due to the applied AC potential at high frequency averts the thermochemical dissociation of the fluid.

4.6 Bio-Micromanipulation Using Magnetic Fields

Biomicrofluidic application involving magnetic forces are abound particularly as trapping and transport mode of magnetically tagged single cells in microchannel system. One main reason for exploiting magnetic field as the manipulator is its comparatively non-lethal effect on biological entities. There have been numerous means by which researchers utilized magnetic field in driving and actuation of microflows [112]. While Micropumps have been fabricated by Magnetohydrodynamic effect, magnetically doped polymer or magnetic materials such as ferrofluids are typically used for valving action. Other important fluidic operations such as micromixing have been performed by the regulated oscillation of magnetic microparticles in a two-fluid stream. From the biomicrofluidics perspective, magnetic particles have been used as solid supports for assaying bioreaction which are essentially integrated with magnetic system detection on lab-on-a-chip scale. Following, we will discuss major microfluidic methods involving magnetic field based manipulation.

4.6.1 Magnetic Field Flow Fractionation (MFFF)

Pioneered by Giddings et al. [83, 113], MFFF has since become well-utilized method for separation which fundamentally exploits the differences in magnetic susceptibility among various components in a mixture. Multifarious applications of MFFF have been appreciated in the realm of separating colloids, particles, and biological macromolecules including proteins and even, cells. Mechanistically, the operation principle of MFFF is very similar to other field flow fractionation variants with magnetic force standing as the major driving impetus. In MFFF systems, the wall-directed transverse magnetic force is counter-balanced by the diffusion and time-invariant suspended particle distribution is achieved. Subsequently, subjected to longitudinal hydrodynamic force, these particles traverses longitudinally according to the velocity distribution across the channel cross-section. As particles with different magnetic susceptibilities, thereby magnetic forces, attain different height locations, they experience different magnitudes of flow velocity and are

consequently separated. Smaller component thickness yields to more significantly retained fractions and therefore longer elution times. In MFFF, to represent the separation, a dimensionless retention parameter λ [114] is defined which is related to the properties of the particles by

$$\lambda = (4d/w) (k_B T / \mu \Delta H)^2 \quad (4.57)$$

Where d , w , μ and ΔH are the particle diameter, capillary diameter, magnetic moment and drop of magnetic field across the capillary respectively. k_B is the Boltzmann's constant.

The most generic chemical means of synthesizing monodisperse magnetic particle is the thermal reduction of organometallic precursor comprising of pure metals such as Iron, Nickel, Cobalt as well as composites such as CoFe_2O_4 , FePt_3 and MnFe_2O_4 . Acetylacetonate has been the most commonly used organic group. Subsequently, synthesized particles are stabilized by organic ligands such as organic acid groups, amine terminated alkanes or phosphine oxide. Further, these conventionally used magnetic nano-particles being water insoluble and in some cases, bio-incompatible, researchers have developed synthetic protocol for obtaining water soluble monodisperse magnetic particle by using MFFF method. This technique is very distinctive in comparison to electromagnetophoresis, where a magnetic field applied at right angles to an electrical current, influences the migration of nonmagnetic and neutral particles perpendicular to the current.

4.6.2 Magnetic Biomaterials

Most of the biological entities such as DNA, proteins, cell and other biologically relevant polymers are diamagnetic in nature. All materials are categorized, according to their magnetic susceptibility χ , into three broad magnetic classes namely diamagnetic, paramagnetic and ferromagnetic. Diamagnetic or nonmagnetic materials generally move opposite to the direction of magnetic field. In contrast, paramagnetic and ferromagnetic materials align themselves to the direction of net magnetic field [115]. In biology, a subclass of paramagnetic materials called supermagnetic particles is used very frequently. Supermagnetic particles generally consist of iron oxide crystal core and coated with polymer materials derivatized to produce free amine or carboxyl groups which may be tuned towards the exploitation of a particular biochemistry. For example, biological macromolecules such as proteins, DNA, mRNAs (messenger ribonucleic acids) can be tagged with such supermagnetic particles [112]. Subjected to a directional magnetic field, these bio-entities can be moved to the desired location. For magnetic manipulation of biological cells, particular cell specific surface protein markers are tagged with supermagnetic particles by antigen-antibody bonding which are effectively irreversible coupling with equilibrium constant value of 10^{14} . Of all commercially available supermagnetic substances, Dynal beads are the most popular from lab-on-a-chip scale application

point of view, attributed to their inherent mono-dispersity in shape and size distribution. Dynal beads have, for the first time, enabled magnetic separation technology and have immediately generated fathomless possibilities for astounding variety of applications within the life sciences, biotech and healthcare. Functionally, these beads are supermagnetic particles tagged with cell-surface-marker specific antibodies. Presently several variants of dynal beads are available all of which are designed towards some targeted cell populations of mammalian immune system. To cite few examples, Protein A, Protein G, Mouse T-Activator CD3/CD28, Human T-Activator CD3/CD28, Human CD4, Human CD8, Human CD3, Mouse PanT, Mouse CD43, Human B Cells, Human Natural Killer Cells, Human Monocyte specific dynal beads are of wide use. In a mixed population of cells, generally isolated from blood sample as in pathological laboratories, cell specific dynal beads will segregate targeted cell types very conveniently. While labeling with magnetic particles of micron or nanometer size has been a plethora in biomicrofluidic assays, it must be mentioned that there are two specific cell types namely Red Blood Corpuscles (RBC) and Magnetotactic Bacteria which are intrinsically magnetic owing their special internal constitution and therefore, have found pertinent microfluidic applications.

4.6.3 Ferrofluids

From microfluidic applications, supermagnetic fluids or ferrofluids are probably the most suitable magnetic materials due to their fluid nature. Essentially they are suspensions of magnetic nanoparticles in water or in organic solvent and are coated to surfactant molecules. Surfactant coating inhibits particle aggregation, maintaining a homogenized magnetic behavior over a large length scale. Ferrofluids being stable hydrodynamically as well as magnetically over a wide range of shear and magnetic field strength, they render exquisite means of exploring the magnetohydrodynamics in lab-on-a-chip scale. The force experienced by the particles suspended in solution system is a strong function of the difference between susceptibilities (χ) between the particle and the bulk medium (commonly water), the absolute strength of the applied magnetic field (B) as well as its spatial gradient. Moreover, the force is directly proportional to the volume of the particle and can thus formulated as,

$$F_p = \frac{(4/3)\pi r_p^3 \cdot \Delta\chi}{\mu_0} (B \cdot \nabla) B \quad (4.58)$$

From the Eq. (4.58), it is very much evident that in a spatially homogeneous magnetic field, zero force is exerted on ferrofluids even if they are strongly magnetized. Microfluidic system with spatially variable magnetic is therefore employed in ferrofluid based lab-on-a-chip devices.

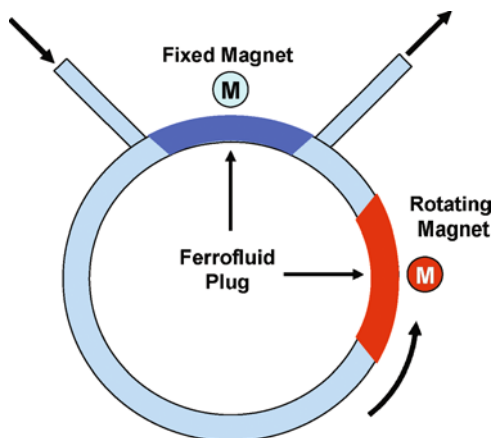
4.6.4 Magnetohydrodynamic Micropumps

Magnetohydrodynamic (MHD) pumps work on the principle of Lorentz force in mutually perpendicular electro-magnetic system [116]. Generically, micropump components consist of conducting fluid as the working liquid, which is subjected to electric and magnetic fields along the width and the height of the microchannel, moves longitudinally due to the Lorentz force. Compatible to any shape of microchannel geometry, flow rates through MHD pumps are conveniently regulated by tuning the externally applied electric and magnetic fields. MHD pumping is appropriate for any conducting liquid and moreover, does not necessitate any moving component. However, for specific applications, integrated switching circuits which can alter the magnitude and direction of the electro-magnetic fields may be incorporated. There is of course another class of MHD pumps which are operated by enclosing the movement of a plus ferrofluid in a moving magnetic field (Fig. 4.10). In this system, the immiscibility between organic ferrofluid solvent and the aqueous solution medium is used to segregate between pumping and transported liquid components. In a pioneering development, researchers [117, 118] have manufactured a circular shaped ferrofluidic micropump essentially consisting of two Nd magnets and two plugs of ferrofluid. One plug is held in a fixed location between the inlet and outlet channel while another plug is circulated by a rotating external magnet. Complementary merge and separation of two plugs in single cycle of plus revolution around the circular pump circuit enables pumping in and out of liquid solutions [119]. Further, very recently, Atencia and Beebe [120] have proposed a MHD pump based on the biomimetics of vortices generated in narrow fluidic confinements by various animals for swimming or flying. Uniquely, this design exploits the biological systems where pumping action is achieved with minimal energy expenditure. Mechanistically, a magnetic bar integrated into a microfluidic structure has been fixed by photolithographically fabricated microposts and the bar is suitably oscillated during operation to create vortices of required strength. In an important biomicrofluidic advancement, West et al. [121] have juxtaposed circular MHD micropump components with on-chip polymerase chain reactions (PCR) using concentrated buffer solutions.

4.6.5 Magnetic MicroValves

Magnetically derivatized or doped PDMS are mostly used for microvalving action [122]. Iron powders with intense magnetic properties are suspended into the base solution of polydimethylsiloxane precursor and thin membrane are then fabricated from it. When these membranes are exposed to the integrated and controllable electromagnetic field, they are deformed. This phenomenon is judiciously engineered in microfluidic circuits to attain the required valving operation. In magnetic valving system, advantageously, no physically moving part is obligatory.

Fig. 4.10 Working mechanism of a representative ferrofluid micropump



4.6.6 Mixing Devices

Magnetic mixing devices work very much identical to the MHD pumps with oscillating magnetic bar system. Pioneeringly introduced to enhance the efficiency and transport kinetics in microchannel based DNA hybridization system by augmenting the mixing of DNA solution with hybridization buffer, Magnetic micromixing devices since then have attracted research attentions [123]. In this system, one end fixed bars commonly fabricated of magnetic permalloy are oscillated inside a microchannel system to enhance two-fluid mixing. Cycling magnetic field is created by four electromagnets tuned in sinusoidal fashion. Chain of magnetic microparticles, stably bonded together covalently or non-covalently with linker molecule, has also been used as the miniaturized stirring system [124]. It has been demonstrated that magnetic micromixing system comprising of pear-shaped chamber along with semicircular wall indentations performs with highest efficiency.

4.6.7 Magnetic Trapping and Sorting of Biomolecules

Biomolecules such as DNA, protein and entities like cells can be pulled along a magnetic field owing due their inherent characteristics [112]. While moved in spatially variable magnetic field, these objects can be uniquely confined into a particular domain. There have been numerous designs of the magnetic systems integrated with microfluidic network. To cite a few, Tapered electromagnet, sawtooth shaped tapered magnets and mech-type magnets have been extensively used. Here, the objective is to facilitate a ratchet-like motion where magnetic particles are transported from field maximum to another. Several magnetic materials such as magnetic beads, magnetically labeled yeast cells and magnetotactic bacteria have been manipulated using aforementioned arrangements. Recently, functionally similar to optical tweezers, magnetic tweezers have been developed to trap magnetic particles or magnetically tagged biological entities within a very

constricted spatial location, thereby increasing effective concentration. Alongside the magnetic transport and trapping, magnetic field based separation has also been investigated, where differential magnetic susceptibilities among different types of particles stand as the governing principle. Subsequently, in microfluidic systems, separation has been implemented by employing either H-type of filtering design or single channel based retarded system of separation.

4.6.8 Magnetic Particles for Bioassays

Magnetic particles are used for carriers in microfluidic based study of Ligand-Receptor interaction and screening of a cell specific type of Receptors. As a general procedure, magnetic nanoparticles which are dynamically trapped into a desired location, are tagged with Ligand of interest [125]. Subsequently, while receptor molecules or cells containing receptor molecules are transported through this region, they are captured by the magnetic particles. Hence, in principle, magnetic particles function as immobilization matrix; however with an advantage of spatiotemporal controllability of their manipulation. In addition, gifted with intrinsic high surface area to volume ratio, these micron or sub-micron sized particles non-trivially augment the binding rate and the sensitivity of the assay. One of most prolific use of these particles has been anticipated in microfluidics based immunoassays, as demonstrated by Hayes et al. [126]. They have essentially immobilized antibodies over NdFeB magnets and antigen containing sample has been assayed by studying the antigen-antibody binding phenomenon during sample transport through designed glass microcapillaries. Similar studies have been performed for various interleukins (e.g. IL-5), parathyroid hormone, DNA and RNA [112]. A plug of immobilized DNA onto a permanent external magnet embedded within microfluidic circuitry has been used to capture complementary secondary strands which are flushed through the microchannels. Taking advantage of a cluster magnetic particles in a microchannel network, disease specific mRNAs has been isolated from total RNA content with unprecedented capture efficiencies of 50% [127]. Relevantly, isolation of RNAs marking Dengue fever virus in a PDMS based microchip has been also illustrated [128]. With time, magnetically manipulated solid assays have covered the domain of marker specific cell isolation also. For example, an immortalized line of T lymphocytes called Jurkat cells have been separated from whole-blood sample by anti-CD3 tagged magnetic particles having 500–1000 μm radius [129]. The efficiency of isolation has been reported to be approximately 50%. Similar isolation method has also been used for capturing rare circulating T-lymphocytes [130].

4.7 Experimental Approaches

The objective of biomicrofluidics is to miniaturize the lab-scale analytical systems into a size of computer chip. Small device-length scale enables high surface to volume ratio, low sample volume requirement and augmented sensitivity which are

critical requirements for detecting and analyzing low abundance samples. However, this objective has been overshadowed by the lack of dimensionally compatible optical, fluorescence and other detection systems. Till date, commonplace detection systems have been bulky with their size being 10^4 – 10^6 times that of the lab-on-a-chip devices. Hence, even if the process itself has been successfully miniaturized, the detection component still compels voluminous operation. In order to remove this drawback, in recent times, there has been a constant effort of fabricating on chip optical detection systems collectively known as “optofluidics”. However, before we proceed to demonstrate the progresses in the field of optofluidics, let us briefly describe how in principle an optical or fluorescence microscope system works.

4.7.1 *Optical and Fluorescence Microscopy*

The type of microscope that utilizes visible light through a system of lenses in order to produce magnified images is called optical or light microscopes. The produced images are then viewed through eye-piece or captured by charge coupled device (CCD) camera and respectively, transferred into a computer screen. A typical optical microscope system consists of ocular lens or eyepiece, objective lenses, light illuminator, mirror, diaphragm and condenser (Fig. 4.11). An eyepiece is a cylindrical object with typically two or more lenses serially inserted inside to provide required observable focus of image. For convenience, they are placed in the top-portion of

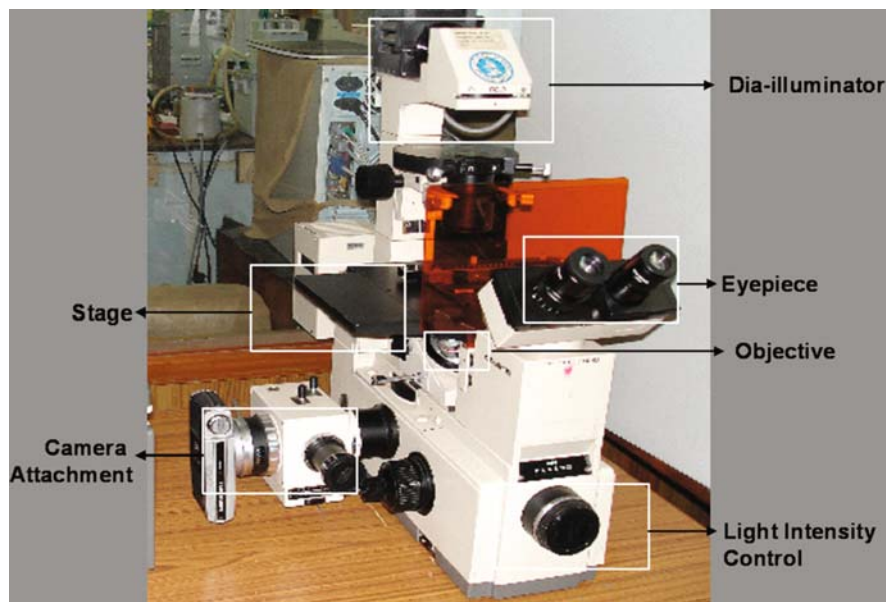


Fig. 4.11 Graphical dissection of an inverted phase contrast optical microscope

an optical microscope and come with 2–10x magnification in tune with the overall optical configuration of the light microscope system. The objective lenses are most important components of an optical microscopy system and are essentially cylinders containing embedded glass lenses to collect light from the sample. With a set of coarse and fine adjustment knob, objective lenses can be moved up and down to obtain the perfect focus of the object to be viewed. Typical objective lenses come with 4x, 5x, 10x, 20x, 40x, 50x and 100x amplification and with several different numerical aperture (NA) values. There is special version of lenses called oil immersion lenses with 50–100x magnification, which facilitate transmission of light from specimen to objective with minimal dissipative refraction. Next, the controllable illumination source which may be a mercury vapor lamp, xenon arc or tungsten halogen lamp, is placed either on the top (as in case of reflection microscope) or the bottom (as in case of inverted microscope) of microscope stage. Light coming from the source is then focused through an optical condensers, diaphragms and filters to produce variable quality and intensity. Optical microscopes have several variants including phase contrast, differential interference contrast (DIC) and stereo types. While phase contrast and DIC types are suitable to selective visualization of biological objects within different optical density than the bulk solution, stereomicroscopes are typically used to obtain a whole-device image of microfluidic systems. Compound optical microscopes are capable of constructing even 1000x magnified image of a specimen.

The resolving power or the resolution of an optical microscope is defined as the minimum distance between two neighboring airy disks due to diffraction, for which each of the disk can be effectively distinguished from it neighbor. This, in other way, represents the ability to resolve fine structural details. For an illuminating light with wavelength λ and objective with numeral aperture NA, the resolution is formulated as

$$d = \frac{\lambda}{2NA} \quad (4.59)$$

which for normal visible light falls in the range of 200–300 nanometers.

A normal brightfield microscope is limited by quite poor contrast as the refractive indices cell sample and bulk medium are approximately identically and only when the phase of the light passing through the sample is significantly altered, image is obtained with good contrast. With the unavoidable requirements of detecting a specific molecule or biological entity with a distinguished fluorescent emission, a process which assists sensitive detection with minimal background, fluorescent microscopes have been most essential visual analytic system for biomicrofluidics. In this class of microscopy, the specimen is illuminated with a light of narrow band of wavelengths belonging to a specific color (ultra-violet, blue, green, red) coming through an excitation filter to excite the desired type of fluophore which then emits the light of longer wavelength. For this purpose, either a particular component of the specimen is labeled with a fluorescent molecule such as fluorescein, rhodamine or a molecule e.g. green fluorescent protein (GFP) can be

intrinsically fluorescent. Successively, an emission filter is used to selectively allow the emitted wavelengths. Generic components of a fluorescence microscope comprises of light source, the excitation filter, the dichroic mirror and the emission filter. Every dye comes with its specific range of spectral excitation and emission wavelengths and accordingly, the filters and the dichroic mirrors are selected. Multi-color images of several fluorophores can be constructed by super-imposing single fluorophore images. If the excitation and observation are made from the top the specimen, the microscope system is recognized as epi-fluorescence type. Although fluorescence microscope has enabled high resolution optical imaging, it is generally limited by gradual reduction in fluorescence intensity on exposure to excited light, a phenomenon called photobleaching. However, selective photobleaching and the intensity recovery thereafter are advantageously utilized in a technique called Fluorescence Recovery After Photobleaching (FRAP) [131] which measures the effective diffusion coefficient of a biological component. With time, several fluorescent molecules having reduced photobleaching and enhanced specificity towards a targeted biological or sub-cellular component are being chemically synthesized. In addition to epi-fluorescence microscopy, there are several advanced fluorescence imaging techniques such as confocal, multiphoton microscopy and the recent super-resolution techniques STED and 4Pi which enables visualization at single entity or at even single molecular level.

4.7.2 Confocal Microscopy

While most of the bright-field and fluorescence optical detection systems fulfill the need for biomolecular phenomena occurring within microconfinement, they are strongly impeded by their inability to resolve structures in z-dimension. This becomes specifically indispensable when the pattern flow or dynamics of biological entities is required to be monitored at three dimensional scales [132]. For example, there may be special microfluidic designs of fluidic components such as valves, pumps etc. whose operation principle takes advantages of every dimension. In this case, though planar two dimensional views may be elucidated by conventional optical detection system, the visualization of flow structure in third dimension remains unfortunately impaired. Also, complex high-throughput microfluidic system may be compiled of different component fabricated at multiple layers and thus, necessitates three dimensional visualization systems with capability of exclusively resolving the events occurring at each layer. Moreover, for microfluidic systems, in general, accurate characterization of device form holds the key for successful operation. Microfluidic devices characteristically contain an array of microfabricated components including channels, valves, pumps and mixers. The capacity to determine and control the dimensional design of these structures is a crucial obligation, not only to guarantee the functionality of operating devices, but also to offer a fundamental means for inventing and improving novel designs. From these very needs, depending upon the explicit rationale, laser scanning confocal microscopy has discovered many relevant applications in the realm of biomicrofluidics.

A confocal microscope system exploits a point illumination and a pinhole in an optically aligned plane in front of the electronic detector in order to diminish the out-of-focus or rather out-of-plane emission. Essentially, confocal microscopes possess a very low depth of focus. As they are integrated with highly-sensitive sensor coupled motorized system along each of x, y and z axis, image data from exclusively each focal plane can be conveniently accessed. In commercial confocal microscopy systems, highly collimated laser light sources of a specified wave-length and extremely narrow spectral spread, are transported along optical fibers to the specimen location. Operationally, only one point (or pixel in image notation) of the specimen being illuminated and imaged at a time, two or three dimensional imaging over a finite specimen section imposes sequential scanning over a regular raster-tracks in the specimen. This fundamental limitation impedes the rapidity of data acquisition which is a decisive factor governing the performance and efficiency of microfluidic systems. Relevantly, in recent times, fast scanning spinning or Nipkow disk confocal microscopes have been invented. The disk is composed of multiple pinhole-like apertures and it spins swiftly over the microscope stage in such as way each aperture traces a linear path through the image. A photosensitive detector collects data from each aperture, which are then assembled by computer program in form a image. Thus, advanced confocal imaging with spinning disk mechanism and multiple confocal apertures are capable of unleashing a high degree parallel data processing mechanism for image acquisition at an unprecedented speed.

The use of confocal microscopy as a detection system for biomicrofluidics has opened up a vast range of molecular experimentations of which Fluorescence Recovery After Photobleaching (FRAP) and Förster Resonance Energy Transfer predominantly worth definite emphasis. In FRAP [133], fluorescence intensity of a small region of the sample, referred as region of interest or ROI here in after, is bleached with high intensity ($\sim 1\text{--}20$ mW) laser pulses. As the fluorescent molecules from neighboring region move into the ROI by the virtue of intrinsic diffusion, the ROI intensity get replenished to some extent (Fig. 4.12). Subsequently, analyzing the dynamics of fluorescence recovery in tune with trend predicted by transport equations, the effective diffusion coefficient (D_{eff}) can be determined. In biological systems where it is extremely unfeasible to decouple advective and diffusive parts of transport mechanism, D_{eff} empirically represents their compounded effect. The fluidity of a cellular component such as cell membrane or cytosol is then directly correlated with acquired D_{eff} .

FRET technology explores resonance energy transfer between two compatible fluophores by an inter-molecule dipole-dipole interaction mechanism and is used to assess the Ligand-Receptor binding and the coupling reaction kinetics at the molecular level. In a generic FRET assay [134], donor fluophore is excited, which then transfers its energy to its acceptor counterpart and emission characteristic of acceptor fluophore is recorded. As the dipole-dipole interactions are effective within only few nanometers of molecular separation, the energy transfer occurs only when molecules are in close-proximity typically encountered during binding or reaction.

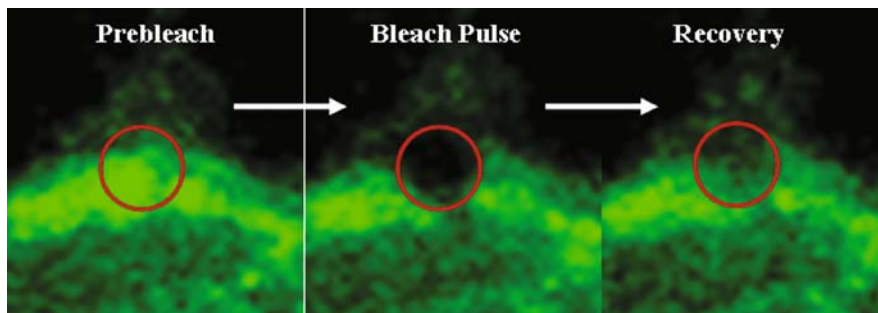


Fig. 4.12 Schematic representation of FRAP technology. Cells have been grown inside microchannel network for 36 hours and labeled with membrane binding carbocyanine dye DiO

In order to explore the fundamental biophysics at the single-molecule level, researchers have invented an enormously high resolution technology based on the low-background and narrow field-depth of evanescent waves. This observatory technology, known as Total Internal Reflection Fluorescence Microscopy (TIRFM), has enabled visualization down to single molecule length scale. Interestingly, owing to its intrinsic ability to resolve close-to-the-surface interfacial phenomena, the TIRFM system has been advantageously utilized in revelation of liquid slip length over a hydrophobic microchannel surface with nanometer resolution [135, 136].

4.7.3 Optofluidics

The classes of optical systems that are integrated with or synthesized of fluids are known as optofluidics [137, 138]. The technology has stemmed from the requirement of fabricating an optical detection system dimensionally commensurate with the micron-sized device itself. The high resolution imaging constraint in conventional microfluidic systems nullifies the cost-size benefits of micro-analytical systems. The most convenient solution in this respect is to integrate sensor-aperture arrays and possibly, illumination sources into the device itself. In principle, the detection parts are fabricated separately and then, coupled with the polymer based microfluidic device as a separate operational layer. With respect to the built-in materials, the optofluidics is broadly classified in three main categories – liquid-in-solid, liquid-in-liquid and systems. Liquid-solid systems work on the principle of highly contrasting refractive indices and total internal reflection in the interface which can be judiciously maneuvered to fabricate in situ diaphragm based lenses and optical-fiber like wave-guides. Moreover, within the domain of microfluidic technology, the focal length of adaptive integrated lenses can be dynamically manipulated by attenuating hydrostatic pressure on the diaphragm surface. A periodic array of voids where each void is selectively filled with absorbing dye can be utilized to manufacture any arbitrary shaped two-dimensional pattern. Another example of liquid-solid optofluidics technology, on-chip compact interferometer has been used as biosensors and

chemical analyzers. Optofluidic devices that rely on evanescent-wave propagation can also perform as surface-plasmon sensors. High-Q resonators and the zero-mode waveguide sensors also belong to the class of liquid-solid optofluidic systems. In liquid-in-liquid systems, the total internal reflection between two immiscible liquid is utilized as the optical wave-guides with liquid-core and liquid-cladding. In low Reynolds number regime of microfluidics, flows are predominantly laminar and the liquids injected in parallel fashion continue to move side by side without any appreciable mixing. Now, if there exists a significant disparity of refractive indices between two liquids, transmitted light can effectively be confined within the domain encompassed by the liquid with lower refractive property, essentially yield a liquid form of optical cable which is then manipulated for in situ visualization and optical detection. The remaining class of optofluidic systems i.e. solid-in-liquid is mostly encountered when solid particles are dispersed within the bulk liquid and resulting localized gradients in optical properties serve as the underlining working ingredient. One popular example is the optical trapping of colloidal particle and biological cells where a highly focused beam of light is utilized to trap and move the suspended materials. In conjunction, researchers have also developed extremely sophisticated microfluidic devices including quantum dot based enhanced Raman scattering fluidic systems and fluidic memory devices.

4.7.4 Flow Visualization

Perhaps, for the subject of microfluidics which aims towards producing smaller and faster assay devices, the most essential and fundamental information is the complete knowledge of spatiotemporal pattern of fluid flow [139]. As a result of the radical declination in length-scales associated to miniaturization, microflows differ extensively from conventional macroscale flow theories with the incipient domination of extended interfacial phenomena. Thus, the prime objective of microscale flow visualization is to acquire the flow profile within designed fluidic circuits. The situation can be extremely interesting and non-intuitive if the flow is significantly perturbed by the presence of deformable biological objects such as cells. Theoretical investigations have demonstrated that in presence of dimensionally commensurate obstacles, surface stresses can be amplified in non-trivial manner. Till date, bulk of the microscale flow visualizations have been particle based of which microscale particle image velocimetry (μ PIV) has been the most dominant type. In this system, the velocity vectors are computed by determining the displacement of dispersed particles between two successive time frame images [140]. The displacement calculation algorithm relies upon determining the peaks in averaged correlation landscape. Other particle based flow visualization techniques include particle streaking method where particle movement lines are delineated with finite time exposure during image acquisition [141] and Laser Doppler Velocimetry (LDV) [142]. In order to meet the criterion of using nanometer sized tracer particle compatible to cause least flow disturbance, one of the major challenges in particle based

microflow visualization remains to eliminate the noise due to the enhanced relative contribution of stochastic Brownian motions in effective displacement [143]. In simultaneous advancements, scalar methods of microflow visualization which are primarily designed towards deciphering the flow patterns typically occurring during micromixing, flow instability and flow transformation, have been progressively developed. Here, the underlining principle is to either excite or bleach a strip-like fluid segment spanning across the microchannel cross-section and investigate the gradual deformation of the strip with time. For this purpose caged-fluorescence molecules and molecules with controllable bleach properties have been extensively used. While two-dimensional flow profiles are non-tedious to characterize, imposing challenges still persist in quantitative flow visualization in three dimensional forms and confocal based μ -PIV promises to solve pertinent hindrances [144, 145].

4.7.5 Non-Optical Detection

They say “seeing is believing” and while optical sensing techniques constitute the most common and form of detection module, these are predominantly limited by the inability to distinguish features below the wavelength of visible light spectrum. Optical signals because of their propagation in all directions, are generally collected in weak intensity and are needed to be amplified for satisfying all practical purposes. Moreover, from the optical measurement, it is very difficult to determine the number of targeted molecules actually present. With the background of these drawbacks in conjunction with the superfluous requirement of bulky optical microscopy components, the non-optical detection techniques for detecting very trace amount of desired specimens have gained increasing applications. In this clan of detection systems, there exists an array of integrated sensors which acquire and transmit some kinds of physical property changes in response to a chemical alteration in their vicinity. For the simplest of examples, if a molecule binds to an electronic sensing unit, it changes the conductivity, the resistance and the capacitance of the sensor, any of which can then be measured with auxiliary electronic circuits. In recent times, the performance and sensitivity of such element have been drastically augmented by implementing nanotubes or nanowires as the working segment. Specifically in applications related to on-chip DNA hybridization, nanowire based detection systems are of high demand.

Relevantly, macroscale high-end chemical detection methodologies such as Raman Spectroscopy have been miniaturized into a microfluidic confocal Raman spectroscopy device to impart the ability of performing local chemical detection and qualitative-quantitative analysis for various species present in infinitesimal amount. Other non-optical probing techniques such as atomic force microscopy (AFM) system have been quite functional in this respect [146]. Fundamentally, the deflection of the AFM probe with different forces has been used to examine the torsional force-velocity interrelation with reduced noise level and the non-intuitive consequences of the forces whose relative manifestation is appreciated exquisitely within micro-confinements. Label free methods of detection [147] such as those utilizes total

internal reflection fluorescence microscopy (TIRFM) technology, Mach-Zehnder interferometer (MZI) and cantilever based biosensors [148] have also found their application in the realm of biomicrofluidics. However, challenges still remain pertaining to the limit of detection, precision, applicability and reproducibility of these biosensors.

4.8 Concluding Remarks

In the last 15 years or so, microfluidics has thrown its fathom in every corner of biology, in order to exploit the physico-chemical events at the level of single biological entities with unprecedented resolution, precision and elaboration. In the aforementioned sections, we have attempted to delineate the glimpse of technology, its elemental root, the governing dynamics and the future perspectives. It is to be summarized that the progresses in biomicrofluidic technology have been predominantly projected towards yielding lab-on-a-chip type appliances possessing enhanced device performance, increasing parallelization and augmented response. Simultaneously, there has been a parallel look out for fundamental sciences which are manifested only at the length-scale of microconfined domains. In this journey, there remain several challenges which biomicrofluidics must circumvent if its vistas are to be expanded in future. These include biocompatibility of microfluidic devices, sustenance and biochemical perseverance of biological entities within microconfinement and intrinsic limitation pertaining to molecular handling in trace concentration level. Original research endeavors on exploring microscale fluid physics, effect of physical forces on biological dynamics and instrumentation design for appreciating the aforementioned physico-biological correlations in practical dimensions need to be aptly emphasized in order to achieve the challenging feats of realizing biomicrofluidics as a sustainable technology in the future.

References

1. Whitesides GM (2006) The origins and the future of microfluidics. *Nature*. 442:368–373.
2. deMello AJ (2006) Control and detection of chemical reactions in microfluidic systems. *Nature* 442:394–402
3. Squires TM and Quake SR (2005) Microfluidics: Fluid physics at the nanoliter scale. *Rev. Mod. Phys.* 77:977–1026
4. Beebe DJ, Mensing GA, and Walker GM (2002) Physics and applications of microfluidics in biology. *Annu. Rev. Biomed. Eng.* 4:261–286
5. Hong JW and Quake SR (2003) Integrated nanoliter systems. *Nat. Biotechnol.* 21: 1179–1183
6. Melin J, and Quake SR (2007) Microfluidic large-scale integration: The evolution of design rules for biological automation. *Annu. Rev. Biophys. Biomol. Struct.* 36:213–231
7. McDonald JC, Duffy DC, Anderson JR, Chiu DT, Wu HK, Schueller OJA, and Whitesides GM (2000) Fabrication of microfluidic systems in poly(dimethylsiloxane). *Electrophoresis*. 21:27–40

8. Thorsen T, Maerkl SJ, and Quake SR (2002) Microfluidic large-scale integration. *Science*. 298:580–584
9. Wainright A, Nguyen UT, Bjornson T, and Boone TD (2003) Preconcentration and separation of double-stranded DNA fragments by electrophoresis in plastic microfluidic devices. *Electrophoresis*. 24:3784–3792
10. El-Ali J, Sorger PK, and Jensen KF (2006) Cells on chips. *Nature*. 442:403–411
11. Hansen CL, Skordalakes E, Berger JM, and Quake SR (2002) A robust and scalable microfluidic metering method that allows protein crystal growth by free interface diffusion. *Proc. Natl. Acad. Sci. USA* 99:16531–16536
12. Anderson RC, Su X, Bogdan GJ, and Fenton J (2002) A miniature integrated device for automated multistep genetic analysis. *Nucleic Acid Res.* 28:E60
13. Burns MA, Johnson BN, Brahma Sandra SN et al. (1998) An Integrated nanoliter DNA analysis device. *Science* 282:484–487
14. Emrich CA, Tian H, Medintz IL, and Mathies RA (2002) Microfabricated 384-lane capillary array electrophoresis bioanalyzer for ultrahigh-throughput genetic analysis. *Anal. Chem.* 74:5076–83
15. Gu MB, Mitchell RJ, and Kim BC (2004) Whole-cell-based biosensors for environmental biomonitoring and application. *Adv. Biochem. Eng. Biotechnol.* 87:269–305
16. Reyes DR, Iossifidis D, Auroux P-A, and Manz A (2002) Micro total analysis systems. 1. Introduction, theory, and technology. *Anal. Chem.* 74:2623–2636
17. Craighead H (2006) Future lab-on-a-chip technologies for interrogating individual molecules. *Nature*. 442:387–393
18. Janasek D, Franzke J, and Manz A (2006) Scaling and the design of miniaturized chemical-analysis systems. *Nature*. 442:374–380
19. Mao H, Yang T, and Cremer PS (2002) Design and characterization of immobilized enzymes in microfluidic systems. *Anal. Chem.* 74:379–385
20. Ottesen EA, Hong JW, Quake SR, and Leadbetter JR (2006) Microfluidic digital PCR enables multigene analysis of individual environmental bacteria. *Science* 314:1464–1467
21. Verpoorte E (2002) Microfluidic chips for clinical and forensic analysis. *Electrophoresis*. 23:677–712
22. Mijatovic D, Eijkel JCT, and van den Berg A (2005) Technologies for nanofluidic systems: topdown vs. bottom-up – a review. *Lab Chip*. 5:492–500
23. Ng JMK, Gitlin I, Stroock AD, and Whitesides GM (2002) Components for integrated poly(dimethylsiloxane) microfluidic systems. *Electrophoresis*. 23:3461–3473
24. Madou M, Zoval J, Jia G, Kido H, Kim J, and Kim N (2006) Lab on a CD. *Annu. Rev. Biomed. Eng.* 8:601–628
25. Chakraborty D, Gorkin R, Madou M, Kulinsky L, and Chakraborty S (2009) Capillary filling in centrifugally actuated microfluidic with dynamically evolving contact line motion. *J. Appl. Phys.* 105:084904
26. Das S, Das T, and Chakraborty S (2006) Analytical solutions for the rate of DNA hybridization in a microchannel in the presence of pressure-driven and electroosmotic flows. *Sens. Actuators B: Chem.* 114:957–963
27. Das S, Das T, and Chakraborty S (2006) Modeling of coupled momentum, heat and solute transport during DNA hybridization in a microchannel in the presence of electro-osmotic effects and axial pressure gradients. *Microfluid. Nanofluid.* 2:37–49
28. Dolnik V, Liu S, and Jovanovich S (2000) Capillary electrophoresis on microchip. *Electrophoresis* 21:41–54
29. Heller C (2001) Principles of DNA separation with capillary electrophoresis. *Electrophoresis*. 22:629–643
30. Bhattacharyya A and Klapperich CM (2008) Microfluidics-based extraction of viral RNA from infected mammalian cells for disposable molecular diagnostics. *Sens. Actuators B: Chem.* 129:693–698

31. Lion N, Rohner TC, Dayon Loïc et al. (2003) Microfluidic systems in proteomics. *Electrophoresis* 24:3533–3562
32. Hu S, Michels DA, Fazal MA, Ratisoontorn C, Cunningham ML, and Dovichi NJ (2004) Capillary sieving electrophoresis/micellar electrokinetic capillary chromatography for two-dimensional protein fingerprinting of single mammalian cells. *Anal. Chem.* 76: 4044–4049
33. Freire SLS and Wheeler AR (2006) Proteome-on-a-chip: Mirage, or on the horizon?. *Lab Chip.* 6:1415–1423 (2006)
34. Wang YC, Stevens AL, and Han JY (2005) Million-fold preconcentration of proteins and peptides by nanofluidic filter. *Anal. Chem.* 77:4293–4299
35. Wainright A, Williams SJ, Ciambrone G, Xue Q, Wei J, and Harris D (2002) Sample Pre-Concentration by Isotachopheresis in Microfluidic Devices. *J. Chromatogr., A.* 979: 69–80
36. Tan A, Pashkova A, Zang L, Foret F, and Karger BL (2002) A miniaturized multi-chamber solution isoelectric focusing device for separation of protein digests. *Electrophoresis* 23:3599–3607
37. Li Y, Buch JS, Rosenberger F, DeVoe DL, and Lee CS (2004) Integration of isoelectric focusing with parallel sodium dodecyl sulfate gel electrophoresis for multidimensional protein separations in a plastic microfluidic network. *Anal. Chem.* 76:742–748
38. Brivio M, Fokkens RH, Verboom W, Reinhoudt DN, Tas NR, Goedbloed M, and van den Berg A (2002) Integrated microfluidic system enabling (bio)chemical reactions with on-Line MALDI-TOF mass spectrometry. *Anal. Chem.* 74:3972–3976
39. Moon H, Wheeler AR, Garrell RL, Loo JA, and Kim C-J (2006) Integrated digital microfluidic chip for multiplexed proteomic sample preparation and analysis by MALDI-MS. *Lab Chip.* 6:1213–1219
40. Pollack L, Tate MW, Finnefrock AC, Kalidas C, Trotter S, Darnton NC, Lurio L, Austin RH, Batt CA, and Gruner SM (2001) Time resolved collapse of a folding protein observed with small angle x-ray scattering. *Phys. Rev. Lett.* 86:4962–4965
41. Hansen C and Quake SR (2003) Microfluidics in structural biology: Smaller, faster. . . better. *Curr. Opin. Struct. Biol.* 13:538–544
42. Andersson H and van den Berg A (2003) Microfluidic devices for cellomics: A review. *Sens. Actuators B: Chem.* 92:315–325
43. Gmez-Sjberg R, Leyrat AA, Pirone DM, Chen CS, and Quake, S.R (2007) Versatile, fully automated, microfluidic cell culture system. *Anal. Chem.* 79:8557–8563
44. Das T, Maiti TK, and Chakraborty S (2008) Traction force microscopy on-chip: Shear deformation of fibroblast cells. *Lab Chip.* 8:1308–1318
45. Helmke BP and Minerick AR (2006) Designing a nano-interface in a microfluidic chip to probe living cells: challenges and perspectives. *Proc. Natl. Acad. Sci. USA* 103:6419–6424
46. Abhyankar VV, Lokuta MA, Huttenlocher A, and Beebe DJ (2006) Characterization of a membrane-based gradient generator for use in cell-signaling studies. *Lab Chip.* 6:389–393
47. Lee PJ, Hung PJ, Shaw R, Jan L, and Lee LP (2005) Microfluidic application-specific integrated device for monitoring direct cell–cell communication via gap junctions between individual cell pairs. *Appl. Phys. Lett.* 86:223902
48. Lucchetta EM, Lee JH, Fu LA, Patel NH, and Ismagilov RF (2005) Dynamics of *Drosophila* embryonic patterning network perturbed in space and time using microfluidics. *Nature* 434:1134–1138
49. Takayama S, Ostuni E, LeDuc P, Naruse K, Ingber DE, and Whitesides GM (2001) Laminar flows – subcellular positioning of small molecules. *Nature* 411:1016
50. Wang SJ, Saadi W, Lin F, Minh-Canh Nguyen C, and Jeon NL (2004) Differential effects of EGF gradient profiles on MDAMB-231 breast cancer cell chemotaxis. *Exp. Cell Res.* 300:180–189
51. Breslauer DN, Lee PJ, and Lee LP (2006) Microfluidics-based systems biology. *Mol. BioSyst.* 2:97–112

52. Taylor RJ, Falconnet D, Niemisto A, Ramsey SA, Prinz S, Shmulevicha I, Galitski T, and Hansen CL (2009) Dynamic analysis of MAPK signaling using a high-throughput microfluidic single-cell imaging platform. *Proc. Natl. Acad. Sci. USA* 106:3758–3763
53. Becker FF, Wang XB, Huang Y, Pethig R, Vykoukal J, and Gascoyne PR (1995) Separation of human breast-cancer cells from blood by differential dielectric affinity. *Proc. Natl. Acad. Sci. USA* 92:860–864
54. Yang MS, Li CW, and Yang J (2002) Cell docking and on-chip monitoring of cellular reactions with a controlled concentration gradient on a microfluidic device. *Anal. Chem.* 74:3991–4001
55. Brehm-Stecher BF and Johnson EA (2004) Single-cell microbiology: tools, technologies, and applications. *Microbiol. Mol. Biol. Rev.* 68:538–559
56. Maerkl SJ and Quake SR (2007) A systems approach to measuring the binding energy landscapes of transcription factors. *Science* 315:233–237
57. Yager P, Edwards T, Fu E, Helton K, Nelson K, Tam MR, and Weigl BH (2006) Microfluidic diagnostic technologies for global public health. *Nature.* 442:412–418
58. Andersson H and van den Berg A (2004) Microfabrication and microfluidics for tissue engineering: state of the art and future opportunities. *Lab Chip.* 4:98–103
59. Hatch A, Kamholz AE, Hawkins KR, Munson MS, Schilling EA, Weigl BH, and Yager P (2001) A rapid diffusion immunoassay in a T-sensor. *Nat. Biotechnol.* 19:461–465
60. Weiss M, Elsner M, Kartberg F, and Nilsson T (2004) Anomalous subdiffusion is a measure for cytoplasmic crowding in living cells. *Biophys. J.* 87:3518–3524
61. Banks D and Fradin C (2005) Anomalous diffusion of proteins due to molecular crowding. *Biophys. J.* 89:2960–2971
62. Caspi A, Granek R, and Elbaum M (2000) Enhanced diffusion in active intracellular transport. *Phys. Rev. Lett.* 85:5655–5658
63. Brangwynne CP, Koenderink GH, MacKintosh FC, and Weitz DA (2008) Cytoplasmic diffusion: molecular motors mix it up. *J. Cell Biol.* 183:583–587
64. Zhang C, Xu J, Ma W, and Zheng W (2006) PCR microfluidic devices for DNA amplification. *Biotechnol. Adv.* 24:243–284
65. Pal D and Venkataraman V (2002) A portable battery-operated chip thermocycler based on induction heating. *Sens. Actuators A Phys.* 102:151–156
66. Dittich PS and Manz A (2006) Lab-on-a-chip: microfluidics in drug discovery. *Nat. Rev. Drug Discov.* 5:210–218
67. Kang L, Chung BG, Langer R, and Khademhosseini A (2008) Microfluidics for drug discovery and development: From target selection to product lifecycle management. *Drug Discov. Today.* 13:1–13
68. Gao J, Yin XF, and Fang ZL (2004) Integration of single cell injection, cell lysis, separation and detection of intracellular constituents on a microfluidic chip. *Lab Chip.* 4:47–52
69. Huang B, Wu H, Bhaya D, Grossman A, Granier S, Kobilka BK, and Zare RN (2007) Counting low-copy number proteins in a single cell. *Science* 315:81–84
70. Mitchell MC, Spikmans V, and de Mello AJ (2001) Microchip-based synthesis and analysis: control of multicomponent reaction products and intermediates. *Analyst.* 126:24–27
71. Choi CJ and Cunningham BT (2007) A 96-well microplate incorporating a replica molded microfluidic network integrated with photonic crystal biosensors for high throughput kinetic biomolecular interaction analysis. *Lab Chip.* 7:550–556
72. McAllister DV, Wang PM, Davis SP, Park JH, Canatella PJ, Allen MG, and Prausnitz MR (2003) Microfabricated needles for transdermal delivery of macromolecules and nanoparticles: Fabrication methods and transport studies. *Proc. Natl. Acad. Sci. USA* 100:13755–13760
73. Hilt JZ and Peppas NA (2005) Microfabricated drug delivery devices. *Int. J. Pharmaceutics* 306:15–23
74. Chakraborty S and Tsuchiya K (2008) Development and fluidic simulation of microneedles for painless pathological interfacing with living systems. *J. Appl. Phys.* 103:14701

75. Wiggins S and Ottino JM (2004) Foundations of chaotic mixing. *Phil. Trans. R. Soc. Lond. A* 362:937–970
76. Campbell CJ and Grzybowski BA (2004) Microfluidic mixers: From microfabricated to self-assembling devices. *Phil. Trans. R. Soc. Lond. A* 362:1069–1086
77. Di Carlo D, Irimia D, Tompkins RG, and Toner M (2007) Continuous inertial focusing, ordering, and separation of particles in microchannels. *Proc. Natl. Acad. Sci. USA* 104:18892–18897
78. Dutta D, Ramachandran A, and Leighton Jr DT (2006) Effect of channel geometry on solute dispersion in pressure-driven microfluidic systems. *Microfluid. Nanofluid.* 2: 275–290
79. Huiqian Y, Nguyen N-T, and Huang X (2006) Micromixer Based on Taylor Dispersion. *J. Phys.: Conference Series.* 34:136–141
80. Hardt S, Drese KS, Hessel V, and Schönfeld F (2005) Passive micromixers for applications in the microreactor and μ TAS fields. *Microfluid. Nanofluid.* 1:108–118
81. Stroock AD, Dertinger SKW, Ajdari A, Mezić I, Stone HA, and Whitesides GM (2002) Chaotic mixer for microchannels. *Science.* 295:647–651
82. Lin J-L, Lee K-H, and Lee G-B (2005) Active mixing inside microchannels utilizing dynamic variation of gradient zeta potentials. *Electrophoresis* 26:4605–4615
83. Giddings JC, Yang FJF, and Myers MN (1976) Flow Field-Flow Fractionation: A Versatile New Separation Method. *Science* 193:1244–1245
84. Liu G, and Giddings JC (1991) Separation of particles in nonaqueous Suspensions by thermal-electrical field-flow fractionation. *Anal. Chem.* 63:296–299
85. Sant HJ and Gale BK (2006) Geometric scaling effects on instrumental plate height in field flow fractionation. *J. Chromatograph. A* 1104:282–290
86. Chon K, Moon J, Kim S, Kim S-D, and Cho J (2006) Bio-particle separation using microfluidic porous plug for environmental monitoring. *Desalination.* 202:215–223
87. Gale BK, Caldwell KD, and Frazier AB (1998) A micromachined electrical field-flow fractionation (μ -EFFF) system. *IEEE Trans. Biomed. Eng.* 45:1459–1469 (1998)
88. Edwards TL, Gale BK, and Frazier AB (2002) A microfabricated thermal field-flow fractionation system. *Anal. Chem.* 74:1211–1216
89. Ristenpart WD, Wan J, and Stone HA (2008) Enzymatic reactions in microfluidic devices: Michaelis-Menten kinetics. *Anal. Chem.* 80:3270–3276
90. Gomez FA (2008) *Biological Applications of Microfluidics*, Wiley-Interscience, New York
91. Starkey DE, Han A, Bao JJ, Ahn CH, Wehmeyer KR, Prenger MC, Halsall HB, and Heineman WR (2001) Fluorogenic assay for β -glucuronidase using microchip-based capillary electrophoresis. *J. Chromatograph. B.* 762:33–41
92. Schilling EA, Kamholz AE, and Yager P (2002) Cell lysis and protein extraction in a microfluidic device with detection by a fluorogenic enzyme assay. *Anal. Chem.* 74: 1798–1804
93. Cohen CB, Chin-Dixon E, Jeong S, and Nikiforov TT (1999) A microchip-based enzyme assay for protein kinase A. *Anal. Biochem.* 273:89–97
94. Yang R-J, Fu L-M, and Lin Y-C (2001) Electroosmotic flow in microchannels. *J. Colloid Interf. Sci.* 239:98–105
95. Ross D, Johnson TJ, and Locascio LE (2001) Imaging of electroosmotic flow in plastic microchannel. *Anal. Chem.* 73:2509–2515
96. Fu L-M, Lin J-Y, and Yang R-J (2003) Analysis of electroosmotic flow with step change in zeta potential. *J. Colloid Interface Sci.* 258:266–275
97. Joo S, Chung TD, and Kim HC (2007) A rapid field-free electroosmotic micropump incorporating charged microchannel surfaces. *Sens. Actuators B: Chem.* 123:1161–1167
98. Wu H-Y and Liu C-H (2005) A novel electrokinetic micromixer. *Sens. Actuators A: Phys.* 118:107–115
99. Oddy MH, Santiago JG, and Mikkelsen JC (2001) Electrokinetic instability micromixing. *Anal. Chem.* 73:5822–5832

100. Studer V, Pépin A, Chen Y, and Ajdari A (2002) Fabrication of microfluidic devices for AC electrokinetic fluid pumping. *Microelectronic Eng.* 61–62:915–920
101. Kandlikar SG, Garimella S, Li D, Colin S, and King MR (2006) Heat transfer and fluid flow in minichannels and microchannels, Elsevier, Amsterdam
102. Gao J, Xu J, Locascio LE, and Lee CS (2001) Integrated microfluidic system enabling protein digestion, peptide separation, and protein identification. *Anal. Chem.* 73:2648–2655
103. Doh I and Cho Y-H (2005) A continuous cell separation chip using hydrodynamic dielectrophoresis (DEP) process. *Sens. Actuators A: Phys.* 121:59–65
104. Kang KH, Xuan X, Kang Y, and Li D (2006) Effects of dc-dielectrophoretic force on particle trajectories in microchannels. *J. Appl. Phys.* 99:064702
105. Kua CH, Lam YC, Rodriguez I, Yang C, and Youcef-Toumi K (2007) Dynamic cell fractionation and transportation using moving dielectrophoresis. *Anal. Chem.* 79:6975–6987
106. Cho SK, Moon H, and Kim C-J (2003) Creating, transporting, cutting, and merging liquid droplets by electrowetting-based actuation for digital microfluidic circuits. *J. Microelectromech. Syst.* 12:70–80
107. Fair RB (2007) Digital microfluidics: is a true lab-on-a-chip possible? *Microfluid. Nanofluid.* 3:245–281
108. Sigurdson M, Wang D, and Meinhart CD (2005) Electrothermal stirring for heterogeneous immunoassays. *Lab Chip.* 5:1366–1373
109. Feng JJ, Krishnamoorthy S, and Sundaram S (2007) Numerical analysis of mixing by electrothermal induced flow in microfluidic systems. *Biomicrofluidics.* 1:024102
110. Feldman HC, Sigurdson M, and Meinhart CD (2007) AC electrothermal enhancement of heterogeneous assays in microfluidics. *Lab Chip.* 7:1553–1559
111. Ng WY, Goh S, Lam YC, Yang C, and Rodríguez I (2009) DC-biased AC-electroosmotic and AC-electrothermal flow mixing in microchannels. *Lab Chip.* 9:802–809
112. Pamme N (2006) Magnetism and microfluidics. *Lab Chip.* 6:24–38
113. Mori S (1986) Magnetic field-flow fractionation using capillary tubing. *Chromatographia.* 21:642–644
114. Latham AH, Freitas RS, Schiffer P, and Williams ME (2005) Capillary magnetic field flow fractionation and analysis of magnetic nanoparticles. *Anal. Chem.* 77:5055–5062
115. Doyle PS, Bibette J, Bancaud A, and Viovy J-L (2002) Self-assembled magnetic matrices for DNA separation chips. *Science.* 295:2237
116. Jang J and Lee SS (2000) Theoretical and experimental study of MHD (magnetohydrodynamic) micropump. *Sens. Actuators A: Phys.* 80:84–89
117. Hatch A, Kamholz AE, Holman G, Yager P, and Böhringer KF (2001) A ferrofluid magnetic micropump. *J. Microelectromech. Syst.* 10:215–221
118. Hartshorne H, Backhouse CJ, and Lee WE (2004) Ferrofluid-based microchip pump and valve. *Sens. Actuators B: Chem.* 99:592–600
119. Yamahata C, Chastellain M, Parashar VK, Petri A, Hofmann H, and Gijs MAM (2005) Plastic Micropump With Ferrofluidic Actuation. *J. Microelectromech. Syst.* 14:96–102
120. Atencia J and Beebe DJ (2004) Magnetically-driven biomimetic micro pumping using vortices. *Lab Chip.* 4:598–602
121. West J, Gleeson JP, John A, Collins JK, and Berney H (2003) Structuring laminar flows using annular magnetohydrodynamic actuation. *Sens. Actuators B: Chem.* 96:190–199
122. Jackson WC, Tran HD, O'Brien MJ, Rabinovich E, and Lopez GP (2001) Rapid prototyping of active microfluidic components based on magnetically modified elastomeric materials. *J. Vac. Sci. Technol. B.* 19:596–599
123. Yuen PK, Li GS, Bao YJ, and Muller UR (2003) Microfluidic devices for fluidic circulation and mixing improve hybridization signal intensity on DNA arrays. *Lab Chip.* 3:46–50
124. Biswal SL and Gast AP (2004) Micromixing with linked chains of paramagnetic particles. *Anal. Chem.* 76:6448–6455
125. Verpoorte E (2003) Beads and chips: new recipes for analysis. *Lab Chip.* 3:60 N–68 N

126. Hayes MA, Polson NA, Phayre AN, and Garcia AA (2001) Flow based microimmunoassay. *Anal. Chem.* 73:5896–5902
127. Jiang GF and Harrison DJ (2000) mRNA isolation in a microfluidic device for eventual integration of cDNA library construction. *Analyst* 125:2176–2179
128. Kwakye S and Baeumner A (2003) A microfluidic biosensor based on nucleic acid sequence recognition. *Anal. Bioanal. Chem.* 376:1062–1068
129. Furdul VI, Kariuki JK, and Harrison DJ (2003) Microfabricated electrolysis pump system for isolating rare cells in blood. *J. Micromech. Microeng.* 13:S164–D170
130. Furdul VI and Harrison DJ (2004) Immunomagnetic T cell capture from blood for PCR analysis using microfluidic systems. *Lab Chip.* 4:614–618
131. Reits EAJ and Neeffjes JJ (2001) From fixed to FRAP: measuring protein mobility and activity in living cells. *Nat. Cell Biol.* 3:E145–E147
132. Lima R, Wada S, Tsubota K, and Yamaguchi T (2006) Confocal micro-PIV measurements of three-dimensional profiles of cell suspension flow in a square microchannel. *Meas. Sci. Technol.* 17:797–808
133. Chen Y, Lagerholm BC, Yang B, and Jacobson K (2006) Methods to measure the lateral diffusion of membrane lipids and proteins. *Methods.* 39:147–53
134. Mere L, Bennett T, Coassin P, England P, Hamman B, Rink T, Zimmerman S, and Negulescu P (1999) Miniaturized FRET assays and microfluidics: key components for ultra-high-throughput screening. *Drug Discov. Today.* 4:363–369
135. Huang P, Guasto JS, and Breuer KS (2006) Direct measurement of slip velocities using three-dimensional total internal reflection velocimetry. *J. Fluid Mech.* 566:447–464
136. Huang P and Breuer KS (2007) Direct measurement of anisotropic near-wall hindered diffusion using total internal reflection velocimetry. *Phys. Rev. E.* 76:046307
137. Heng X, Erickson D, Baugh LR, Yaqoob Z, Sternberg PW, Psaltis D, and Yang C (2006) Optofluidic microscopy – a method for implementing a high resolution optical microscope on a chip. *Lab Chip.* 6:1274–1276
138. Psaltis D, Quake SR, and Yang C (2006) Developing optofluidic technology through the fusion of microfluidics and optics. *Nature.* 442:381–386
139. Sinton D (2004) Microscale flow visualization. *Microfluid. Nanofluid.* 1:2–21
140. Santiago JG, Wereley ST, Meinhart CD, Beebe DJ, and Adrian RJ (1998) A particle image velocimetry system for microfluidics. *Exp. Fluids.* 25:316–319
141. McKnight TE, Culbertson CT, Jacobson SC, and Ramsey JM (2001) Electroosmotically induced hydraulic pumping with integrated electrodes on microfluidic devices. *Anal. Chem.* 73:4045–4049
142. Minor M, van der Linde AJ, van Leeuwen HP, and Lyklema J (1997) Dynamic aspects of electrophoresis and electroosmosis: A new fast method for measuring particle mobilities. *J. Colloid Interface Sci.* 189:370–375
143. Wereley ST, Gui L, and Meinhart CD (2002) Advanced algorithms for microscale particle image velocimetry. *AIAA J.* 40:1047–1055
144. Klank H, Goranovic G, Kutter J, Gjelstrup H, Michelsen J, and Westergaard C (2002) PIV measurements in a microfluidic 3D-sheathing structure with three-dimensional flow behaviour. *J. Micromech. Microeng.* 12:862–869
145. Kinoshita H, Kaneda S, Fujii T, and Oshima M (2007) Three-dimensional measurement and visualization of internal flow of a moving droplet using confocal micro-PIV. *Lab Chip.* 7:338–346
146. Anderson MS (2005) Microfluidics and chromatography with an atomic force microscope. *Anal. Chem.* 77:2907–2911
147. Blanco FJ, Agirregabiria M, Berganzo J, Mayora K, Elizalde J, Calle A, Dominguez C, and Lechuga LM (2006) Microfluidic-optical integrated CMOS-compatible devices for label-free biochemical sensing. *J. Micromech. Microeng.* 16:1006–1016
148. Shipper EF, Brugman AM, Dominguez C, Lechuga LM, Kooyman RPH, and Greve J (1997) The realization of an integrated Mach-Zehnder waveguide immunosensor in silicon technology. *Sens. Actuators B: Chem.* 40:147–153